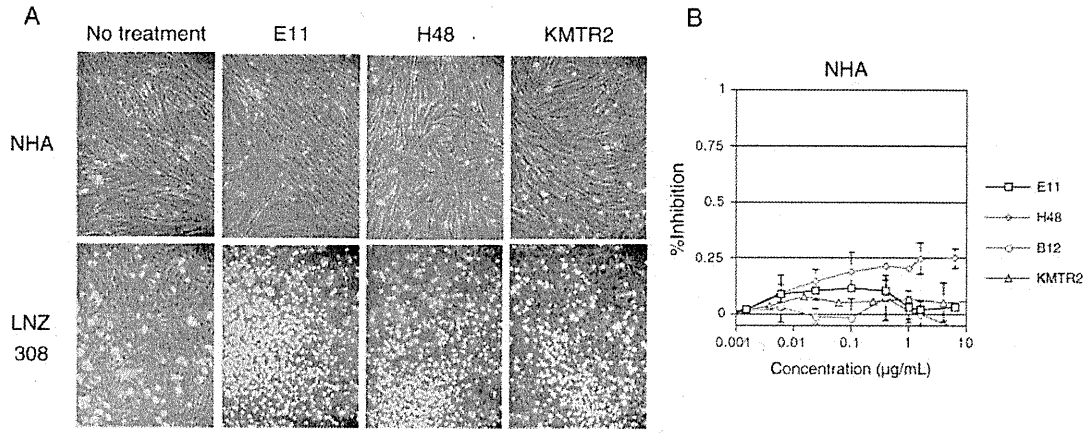

Fig. 3. Fully human anti-DR5 mAbs do not affect viability of NHA. (A) Photomicrographs showing anti-DR5 mAb-induced cytotoxicity in LNZ308 cells, but not in NHA. (B) MTT assay for quantifying cytotoxicity induced by various mAbs against DR4 or DR5 in NHA. Cells were treated with either anti-DR5 mAbs E11, H48, and KMTR2, or anti-DR4 mAb B12 at doses indicated at the bottom of each panel for 48 hours and then were subjected to MTT assays. LNZ308 cells were treated as a positive control for the assay. The experiment was repeated 4 times with the similar results.

family molecules, such as Bcl-X_L, Bax, Bak, and Bid were irrelevant to the sensitivity. Expression of IAP proteins, other cellular apoptosis inhibitors, did not associated with anti-DR5 mAb sensitivity, either. However, the expression of Akt/PKB, which could contribute to tumor cell proliferation and survival, significantly correlated with the sensitivity (E11: $P = .014$, H48: $P = .017$). Furthermore, the expression level of cyclin D1 showed a correlation with the sensitivity as well (E11: $P = .045$, H48: $P = .028$) (Fig. 4C). Among the molecules which were found to be significantly correlated with sensitivity to anti-DR5 mAbs, only the expression of Akt and c-$FLIP_L$ showed a significant correlation ($P = .017$).

Involvement of c-$FLIP_L$ Expression in Sensitivity to Anti-DR5 mAb

As the expression of c-$FLIP_L$, a key regulator at the DISC, significantly correlated with sensitivity to anti-DR5 mAbs in human glioma cells, we downregulated c-$FLIP_L$ expression by using an siRNA specific to human c-$FLIP_L$ mRNA to determine its role in resistance to anti-DR5 mAbs. Transfection of c-$FLIP_L$ siRNA resulted in a significant decrease of c-$FLIP_L$ expression at the protein level in both U87MG and LNZ308 cells (Fig. 5A). Although c-$FLIP_L$ downregulation per se did not affect cell viability, E11 treatment induced robust cell death in those cells with downregulated c-$FLIP_L$, but not in control siRNA treated cells ($P < .001$, t-test) (Fig. 5B).

Alternatively, T98G cells lacking c-$FLIP_L$ expression were introduced with the c-$FLIP_L$ expression vector pCR.FLAG-c-$FLIP_L$, and stable sublines overexpressing c-$FLIP_L$ were obtained (Fig. 6A). As expected, overexpression of c-$FLIP_L$ resulted in remarkable suppression of cytotoxic effects induced by either E11, H48, or sTRAIL when compared with control cells with empty vector (pCR3) transfection (Fig. 6B–F). These results suggested that c-$FLIP_L$ expression confers, at least in part, resistance to anti-DR5 mAbs in human glioma cells, consistent with the good negative correlation observed between the c-$FLIP_L$ expression level and anti-DR5 mAb sensitivity in the panel of human glioma cell lines. Similar results were obtained when T98G cells were forced to overexpress c-FLIPs by transfection with the c-FLIPs expression vector (T98G.c-FLIPs-5, Fig. 6G).

Treatment of Animals Carrying Established Tumor Xenografts with the Anti-DR5 mAbs Causes In Vivo Tumor Regression

We next determined the effect of the anti-DR5 mAb treatment against established tumors. Mice bearing subcutaneous LNZ308 tumor xenografts were treated systemically with E11 for 5 consecutive days as described in the Materials and Methods. The tumors carried by mice treated with E11 grew slower and remained smaller after a course of treatment than those in animals treated with the vehicle control or with the mock control (DNP) (DNP vs. E11: $P < .05$, Mann–Whitney's U-test) (data not shown). As E11 requires crosslinking by effector molecules such as anti-immunoglobulin antibodies for its full apoptotic activity and in in vivo conditions such molecules and/or cells involved in crosslinking are presumably limited to the complement component C1q and Fc receptors present on most immune effector cells,[42,43] we applied another anti-DR5 mAb KMTR2, which has been shown to directly activate apoptosis independent of host effector function.[39] The growth of LNZ308 subcutaneous tumor xenografts were suppressed slightly more by the treatment with KMTR2 (DNP vs. KMTR2: $P < .01$) than by E11 (data not shown). To confirm the possibility that KMTR2 has better antitumor effects in vivo, we

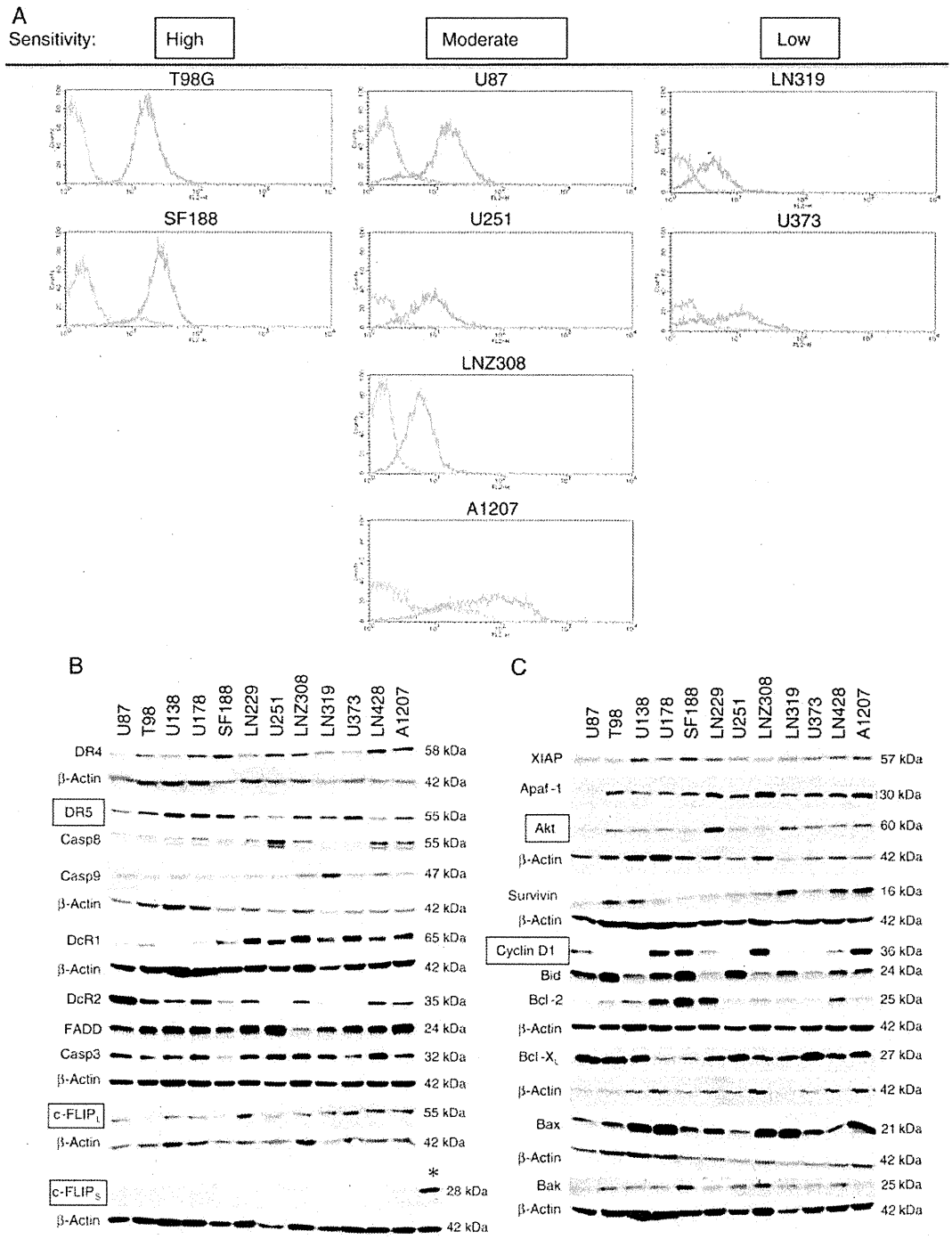

Fig. 4. Expression levels of apoptosis-related molecules in human glioma cell lines. (A) DR5 cell-surface expression determined by flow cytometry analysis. Cultured cells were washed and reacted with PE-labeled anti-DR5 antibody, followed by flow cytometry analysis. Glioma cells with high sensitivity to anti-DR5 mAbs tended to have high cell-surface expression of DR5, whereas those with low sensitivity were associated with low expression. (B and C) Western blot analyses showing expression levels of various apoptosis-related molecules. Human glioma cells were harvested for whole cell lysates, which were then subjected to Western blotting. Expression levels of c-FLIP$_L$, Akt, and cyclin D1 significantly correlated with sensitivity of these cell lines to treatment with anti-DR5 mAbs. Intrinsic expression of c-FLIPs was undetectable in all cell lines tested, whereas exogenous expression of c-FLIPs was identified in T98G.FLIPs cells (indicated as *). The molecules and their molecular sizes are shown on the left and right sides on each panel, respectively.

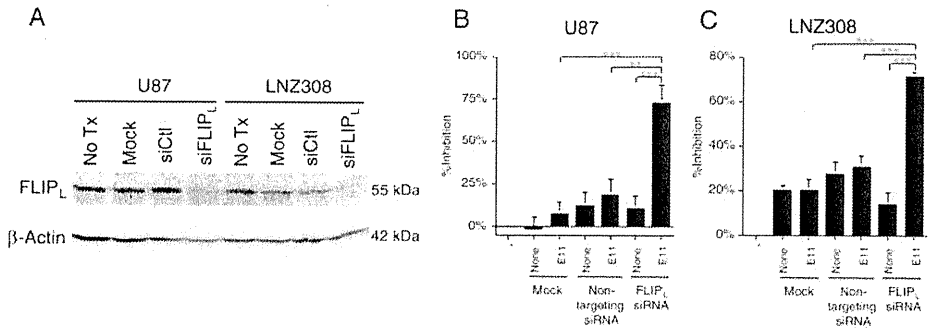

Fig. 5. Downregulation of c-FLIP$_L$ expression sensitizes human glioma cells to anti-DR5 mAb. (A) Western blot showing reduced expression of c-FLIP$_L$ protein upon treatment with siRNA against c-FLIP$_L$ (siFLIP$_L$) in U87MG and LNZ308 cells. Cells were transfected with either nontargeting siRNA (siCtl) or siFLIP$_L$ and were harvested for the preparation of total lysates after being cultured for 48 hours. Twenty micrograms of total lysate was size fractionated in a 10% SDS–polyacrylamide gel, transferred to a PVDF membrane and reacted with a monoclonal antibody against human c-FLIP$_L$. The β-Actin blot demonstrates the loading of lysate in each lane. No Tx, no treatment. (B and C) Enhanced anti-DR5 mAb-induced cytotoxicity by the suppression of c-FLIP$_L$ expression. U87MG (B) or LNZ308 (C) cells were transfected with either siCtl or siFLIP$_L$, followed by treatment with or without E11 at a sublethal concentration (0.01 μg/mL) for 24 hours and then were subjected to the MTT assay. Similar results were obtained when treated with KMTR2. ***$P < .001$, **$P < .01$ (Student's t-test).

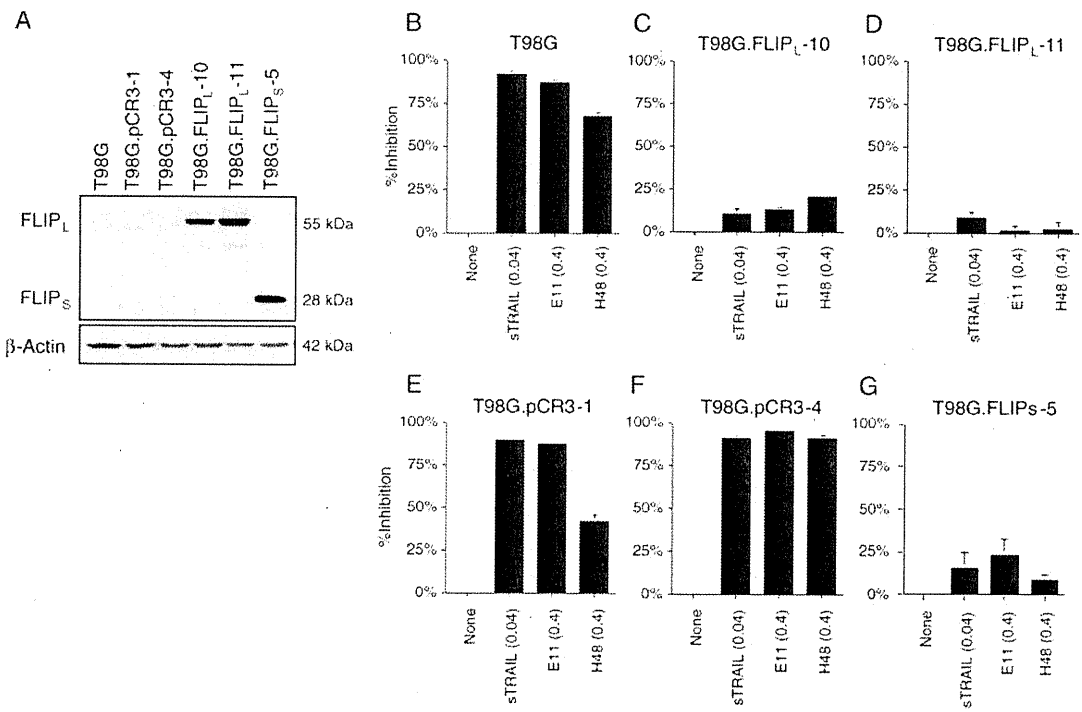

Fig. 6. Overexpression of c-FLIP$_L$ confers resistance to anti-DR5 mAb in human glioma cells. (A) Western blot showing high expression of either c-FLIP$_L$ or c-FLIP$_S$ in T98G.FLIP$_L$-10 and -11, or T98G.FLIPs-5 cells transfected with pCR3.V64-Met-Flag-FLIP$_L$, or pCR3.V62-Met-Flag-FLIP$_S$, respectively, whereas undetectable levels of c-FLIP$_L$ and c-FLIP$_S$ in parental T98G and its subclones T98G.pCR3-1 and -4 cells transfected with the empty vector. (B–G) Suppression of cytotoxic effects by the treatment with anti-DR5 mAbs and sTRAIL in both T98G.FLIP$_L$ and T98G.FLIP$_S$ cells, but not in T98G.pCR3 cells. Cells were treated with either sTRAIL (0.04 μg/mL), E11 (0.4 μg/mL), or H48 (0.4 μg/mL) for 48 hours and then were subjected to MTT assay.

next tested the efficacy of these mAbs to TRAIL-sensitive T98SQ1 xenografts. Mice bearing subcutaneous T98SQ1 tumor xenografts were treated systemically with either E11, KMTR2, or DNP for only 3 days. E11 treatment resulted in the suppression of tumor growth, and even tumor shrinkage for a short period of time. However, KMTR2 treatment lead to complete tumor regression in all mice treated (Fig. 7A). This

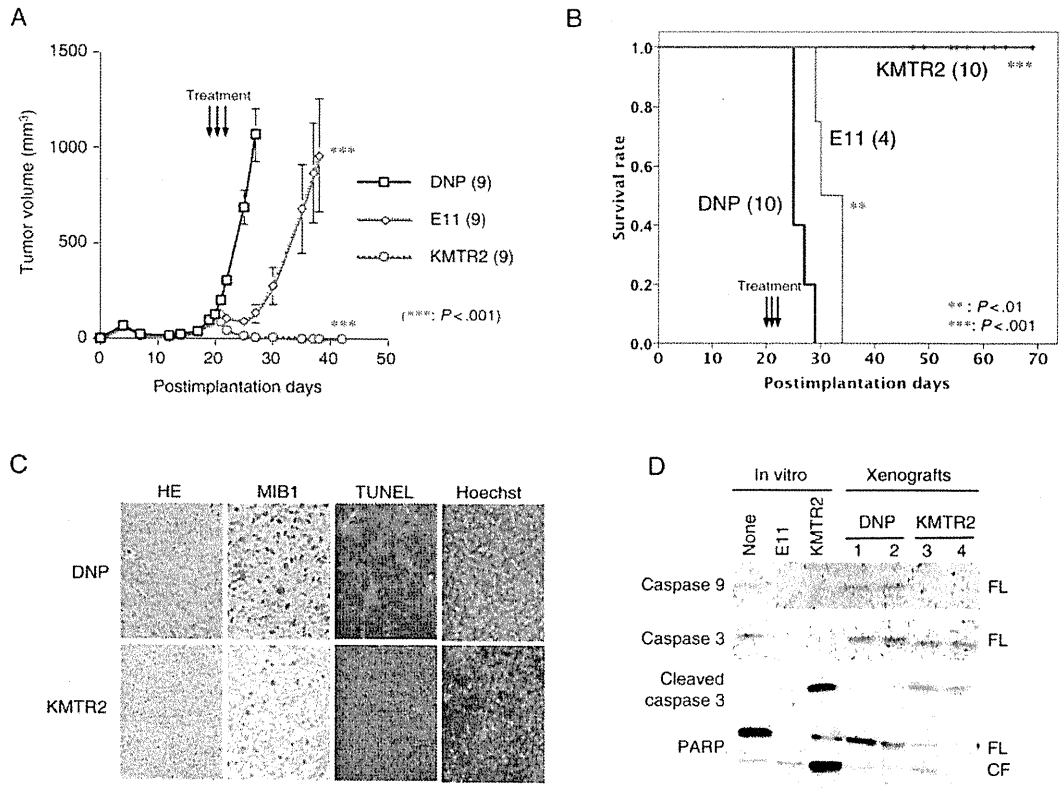

Fig. 7. Tumor regression by treatment with anti-DR5 mAb KMTR2 in vivo. (A) Growth suppression and tumor regression of established T98SQ1 xenografts by fully human anti-DR5 mAbs, E11 and KMTR2, respectively, in vivo. Nude mice (9 per each group) were injected subcutaneously with 2×10^6 T98SQ1 cells and were allowed to establish tumors. From postimplantation Day 20, mice were treated with either anti-DR5 mAb E11 or KMTR2 (5 mg/kg) or control non-specific human IgG (DNP), administered i.p. daily for 3 consecutive days. Square, control DNP; diamond, E11; circle, KMTR2. Data are shown as the mean ± SE. $***P < .001$ (DNP vs E11; DNP vs KMTR2). The experiment was repeated independently 2 times with similar results. (B) Effect of fully human anti-DR5 mAb treatment on survival of mice bearing intracerebral T98SQ1 xenografts. Nude mice were injected intracerebrally with 5×10^5 T98SQ1 cells and were treated from postimplantation Day 20 for 3 consecutive days as described in (A). Mice treated with KMTR2 were sacrificed at various time points and were found to carry no intracerebral tumor at any points. $***P < .001$ (DNP vs KMTR2), $**P = .003$ (DNP vs E11) (log-rank test). The experiment was repeated independently 3 times with similar results. (C) Decreased proliferative activity (MIB-1 index) and increased apoptosis induction (TUNEL positivity) by KMTR2 treatment of T98SQ1 cells in xenografts. Nude mice with established subcutaneous xenografts derived from T98SQ1 cells were treated with either KMTR2 or DNP i.p. for 2 days and were sacrificed on the next day. Tumor tissues were harvested and subjected to either MIB-1 staining or TUNEL assay. (D) Treatment with KMTR2 induces multiple caspase activation in established T98SQ1 xenografts. Tumor lysates were prepared as described in (C) and were subjected to Western blot analyses. Caspase-9, caspase-3, and PARP, a substrate of activated caspase-3, were significantly cleaved upon treatment with KMTR2 but not by control DNP. FL, full length; CL, cleaved form.

striking antitumor effect by KMTR2 was associated with massive apoptosis induction accompanied with a reduced proliferative activity in tumor cells, demonstrated by TUNEL assays and MIB-1 immunostainings, respectively (Fig. 7C). In KMTR2-treated tumors, caspase activation was also detected (Fig. 7D).

We also examined the potency of the anti-DR5 mAb treatments for brain tumors using intracerebral xenograft models. Mice stereotactically inoculated in the brain with T98SQ1 cells were treated with either E11, KMTR2, or DNP for 3 consecutive days. The KMTR2 treatment significantly extended the survival of all mice bearing intracerebral xenografts when compared with either DNP or E11 ($P < .001$) (Fig. 7B). There was only minimum survival benefit by the E11 treatment. Notably, all mice treated with KMTR2 showed no tumor burden when sacrificed at various time points beyond 25 days after treatment, whereas all of those treated with DNP died of tumor within 10 days after treatment. Similar but less survival elongation was observed by these mAbs in mice bearing LNZ308 brain tumor xenografts (data not shown). Body weight of host mice did not significantly change by any types of treatments. These results suggest that anti-DR5 mAbs, especially direct agonist KMTR2, also have potent antitumor effects on brain tumors in vivo.

Association of Relative Resistance of Primary Culture Glioma Cells to Anti-DR5 mAbs with Altered Expression of DR5 and c-FLIP$_L$

As established cell lines may not always represent original characteristics of primary tumors due to long-term culture conditions, we utilized cultures of primary GBM cells at short-term passage numbers and examined their sensitivity to anti-DR5 mAbs in vitro. Primary cultured cells derived from 2 independent glioma tissues did not respond as well to E11 as did the sensitive glioma cell lines by MTT assays (Fig. 8A). These primary cultured cells exhibited higher amounts of c-FLIP$_L$ expression (Fig. 8B) as well as lower levels of cell surface DR5 expression (Fig. 8C), both of which correlated with their sensitivity to the mAb. Furthermore, siRNA-mediated downregulation of c-FLIP$_L$ expression resulted in the enhancement of E11 sensitivity in the primary cultured cells (Fig. 8D), suggesting that the altered expression of these key molecules may, at least in part, account for the resistance.

Discussion

One of the major reasons for the poor prognosis of patients with malignant gliomas is derived from the resistance of these tumors to the chemotherapeutic drugs currently used. Induction of apoptosis through death receptor-mediated intracellular signaling is an intriguing anticancer strategy, especially because of involving signaling pathways directly activating the death executing caspase cascade rather than the mitochondrial damage through which most anticancer therapies operate.[44] Activation of the TRAIL-mediated death signal, among other death-inducing factors, has been intensively investigated both experimentally and clinically because of its advantage as cancer therapeutics

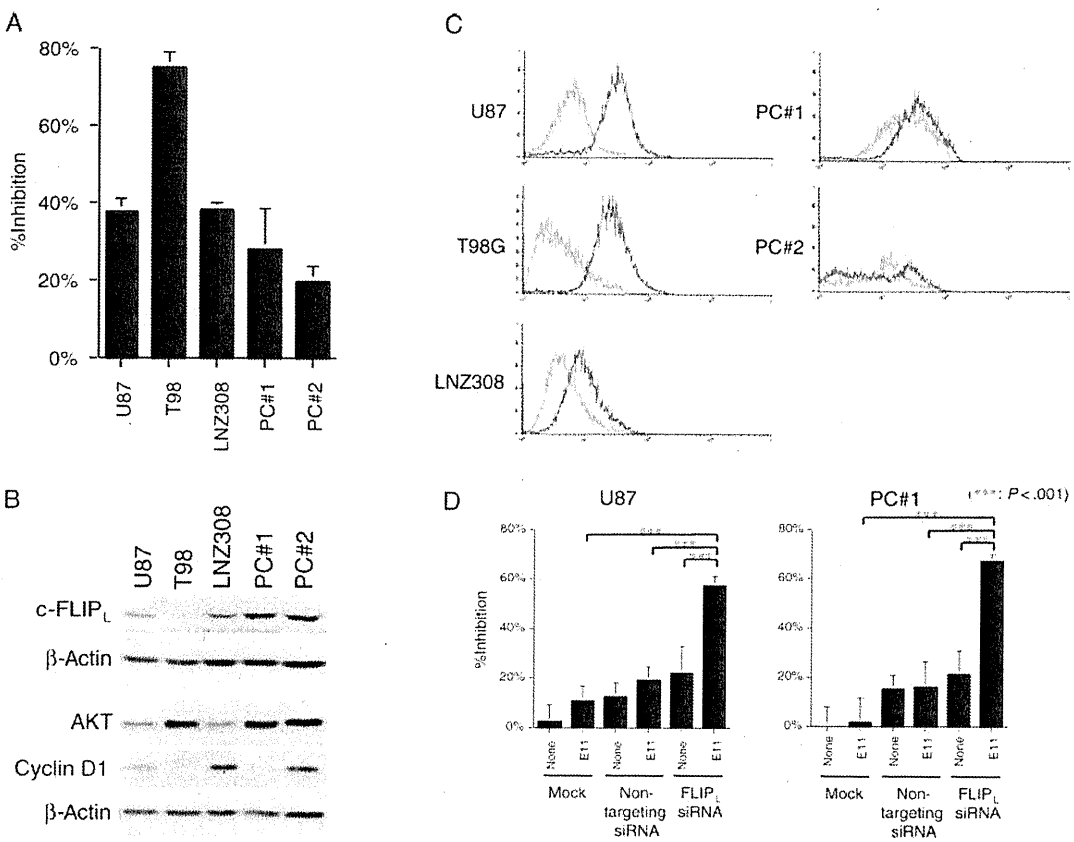

Fig. 8. Association of relative resistance of primary cultures of glioma cells to anti-DR5 mAbs with altered expression of DR5 and c-FLIP$_L$. (A) Primary glioma cells were less sensitive to anti-DR5 mAb than sensitive glioma cell lines. Cells were treated with E11 (0.1 μg/mL) for 48 hours and then were subjected to the MTT assay. The experiment was repeated 3 times with similar results. (B) Western blot analyses showing expression levels of c-FLIP$_L$, Akt, and cyclin D1 in human glioma cell lines and primary glioma cells. Whole cell lysates were subjected to Western blotting and serially probed with the specific antibodies indicated. High expression of c-FLIP$_L$ is observed in primary glioma cells. (C) DR5 cell-surface expression determined by flow cytometry analysis as described in Fig. 4. Primary culture glioma cells tended to have lower cell-surface expression of DR5 than the established GBM cell lines with high sensitivity to E11. (D) siRNA-mediated targeting of c-FLIP$_L$ enhances the sensitivity of primary glioma cells to anti-DR5 mAb. Cells were treated as described in Fig. 5 (E11 at 0.01 μg/mL) and then were subjected to the MTT assay. ***$P < .001$ (Student's t-test). The experiment was repeated 2 times with similar results.

due to preferential targeting of tumor cells but not normal cells. sTRAIL, however, binds to all TRAIL receptors including the death-inducing receptors DR4 and DR5, as well as decoy receptors that do not mediate death signals, rendering its therapeutic spectrum and effects wider or more unpredictable than targeting an individual receptor specifically. Furthermore, some versions of recombinant sTRAIL have been shown to induce differential hepatocyte toxicity.[8,37,38,45] This potential limitation led to the development of proapoptotic mAbs against individual TRAIL receptors,[38,39,46,47] because mAbs restrict the therapeutic target to tumors with a distinct receptor expression profile. The potential therapeutic advantages of using mAb over recombinant sTRAIL to target TRAIL receptors include a longer half-life in vivo, a higher affinity for the target receptor, and no decoy receptor engagement, and they may provide a mechanism to induce long-term, tumor-specific T-cell memory that prevents tumor recurrence.[48]

Here, we show that the fully human mAbs to human DR5, E11, H48, and KMTR2, induced significant cytotoxicity as well as tumor regression in most of human glioma cells through rapid apoptotic induction but did not cause cell death in normal astrocytes. In contrast, anti-DR4 mAb B12, which had been shown to have a potential to affect hepatocyte viability[38] did not induce cell death in all human glioma cell lines, providing support for targeting individual TRAIL receptor by mAbs. In addition, our results that the temozolomide/nitrosourea-resistant T98G and SF188 human glioma cells were highly susceptible to anti-DR5 mAbs suggest that specific targeting of TRAIL receptors could be a meaningful alternative therapeutic strategy to overcome drug resistance.[49] Indeed, agonistic anti-TRAIL receptor mAbs have been currently under intensive investigation, including mapatumumab (HGS-ETR1, anti-human DR4 mAb), lexatumumab (HGS-ETR2, anti-human DR5 mAb), and MD5-1 (anti-mouse DR5 mAb). The former 2 mAbs have been tested in Phase 1 clinical trials in patients with systemic malignancy, exhibiting excellent safety profiles.[36,50–52] Anti-mouse DR5 mAb MD5-1 could also be administered safely without inducing hepatotoxicity either alone or in combination with histone deacetylase (HDAC) inhibitors in mice.[53]

Our findings that human glioma cells were only susceptible to anti-DR5 mAbs but not to anti-DR4 mAb and that their sensitivity to sTRAIL strongly correlated with those to anti-DR5 mAbs suggest that DR5 is the major TRAIL receptor that transduces the death signal in human glioma cells. This might be attributable to the pattern of cell surface expression of TRAIL receptors. Protein expression of both DR4 and DR5 was detectable in all human glioma cell lines tested by Western blot analysis using whole cell lysates, whereas only DR5 was identified to be expressed at the cell surface by flow cytometry. Furthermore, the expression level of DR5 at the cell surface was associated with the sensitivity of glioma cells to anti-DR5 mAb treatment. The reason for the lack of DR4 cell surface expression is yet unclear, leaving room for further investigation including protein trafficking or degradation. The DR5 predilection for TRAIL death signaling in human glioma cells appears to be in agreement with the preclinical experiments, which utilized TRAIL mutants that selectively bind either DR4 or DR5 and have suggested that DR5 might be the more potent receptor for ligand-induced apoptosis of many cancer cell types.[54]

Among human glioma cell lines, some disclosed resistance to anti-DR5 mAb treatment. One of the putative determinants for TRAIL sensitivity includes the expression of the decoy receptors against TRAIL. However, this might not be the case in glioma like other cancers as suggested previously,[55] as we did not see any correlation between the sensitivity to anti-DR5 mAbs and the expression of intrinsic TRAIL decoy receptors. Rather, the glioma cell sensitivity to anti-DR5 mAbs were significantly correlated with expression levels of intracellular intrinsic apoptosis suppressors c-FLIP$_L$ and Akt/PKB. c-FLIP contains a DED, can interact with DED of both FADD and pro-caspase-8 and block upstream caspase activation at the DISC level.[56,57] c-FLIP has thus been implicated in the resistance of cancer cells to apoptosis and is upregulated in some cancer types including Hodgkin's lymphoma, and ovarian and colon carcinomas.[58] c-FLIP is expressed as 2 alternative splice forms, FLIP short (FLIPs) and FLIP long (FLIP$_L$). Both isoforms have been reported to regulate TRAIL sensitivity in a variety of human tumor cell lines.[22,56,58–60] In the glioma cell lines tested, c-FLIP$_L$ expression was nearly absent in T98G and SF188 cells, both of which were the most sensitive to anti-DR5 mAbs. Furthermore, gene transfer of c-FLIP$_L$ into T98G cells resulted in acquired resistance to anti-DR5 mAb treatment. Alternatively, siRNA-mediated downregulation of c-FLIP$_L$ expression markedly sensitized c-FLIP$_L$ expressing glioma cells to anti-DR5 mAbs. These results suggest the expression level of c-FLIP$_L$ as an important molecular determinant, at least in part, of resistance to anti-DR5 mAbs in human glioma cells. Primary cultured glioma cells were also shown to be resistant to TRAIL, which was associated with weak DR5 expression.[61] Accordingly, our results show that the primary glioma cells tended to be less sensitive to anti-DR5 mAb than sensitive established cell lines, which was well correlated with higher amounts of c-FLIP$_L$ expression as well as lower levels of cell surface DR5 expression. Similar to results with the established GBM cell lines, siRNA treatment of c-FLIP$_L$ resulted in the enhancement of E11 sensitivity in the primary culture cells, providing a further rationale to target c-FLIP$_L$ to increase the anti-DR5 mAb sensitivity. Panner et al.[62] reported that c-FLIPs is one of the major intracellular molecules that regulate death signals driven by TRAIL treatment in human glioma cells, as c-FLIPs also targets and inhibits the DISC function. In the human glioma cell lines tested, however, c-FLIPs protein expression was undetectable using several specific antibodies, one of which, albeit, clearly identified exogenously expressed c-FLIPs protein in T98G cells (Figs 4B and 6A), which also conferred resistance to anti-DR5 mAb (Fig. 6G). Although the reason

for lack of c-FLIPs detection at the protein level is not clear, our data indicate that c-FLIP$_L$ could also play a pivotal role in regulating the sensitivity of human glioma cells to anti-DR5 mAb.

In addition to c-FLIP$_L$, protein expression levels of both Akt and Cyclin D1 correlated significantly with the sensitivity of these cell lines to anti-DR5 mAb treatments. Interestingly, there was significant correlation between the expressions of c-FLIP$_L$ and Akt ($P = .017$). Akt plays a key role in transducing survival signals from receptor tyrosine kinases including epidermal growth factor receptor (EGFR) and has been shown to be upregulated in many high-grade gliomas. Panner et al.[62] reported that Akt signaling upregulates the expression level of c-FLIPs through activation of its downstream target mTOR, suggesting a potential connection between Akt and c-FLIP$_L$ status in glioma cells. Overexpression of Cyclin D1 was shown to be associated with the reduced colonization activity by TRAIL in a breast cancer cell line, which had increased expression of DR5.[63] However, the significance of Cyclin D1 expression in the regulation of anti-DR5 mAb sensitivity remains to be elucidated, as there has been no definite evidence of Cyclin D1 transactivation of DR5 expression in human glioma cells.

Treatment of mice bearing human glioma xenografts with anti-DR5 mAbs exerted significant antitumor effects in vivo. E11 monotherapy resulted in reduced tumor volume and suppression of tumor growth, compared with control treatments. However, the response of tumors to E11 remained partial, and there were no complete response and no durable tumor regression obtained. In contrast, monotherapy with another anti-DR5 mAb, KMTR2, exhibited a marked tumor shrinkage leading to complete disappearance and durable remission without recurrence of both subcutaneous and intracranial xenografts derived from TRAIL-sensitive human glioma cells. E11 exists as a monomer, thus requiring an antibody crosslinking to effectively activate death signals that stem from TRAIL receptors. In the athymic mouse body, anti-human IgG (isotype of E11) antibodies are almost lacking, and there are no cytotoxic T cells. In this sense, the cytotoxic action by E11 may be restricted to immune systems except T cells or complement-dependent cytotoxicity which is mediated through the activation of complement system by binding to the DR5–E11 complex and thus could be less effective in inducing robust tumor cell death in athymic mice. On the other hand, even in the milieu where T cells are defective, KMTR2 has a potential to bind to and directly multimerize DR5 leading to the activation of death signals. As a result, KMTR2 was very efficacious in killing tumor cells in vivo compared with E11, demonstrating complete response and durable remission in the animal models. This finding is of great advantage in the application of the anti-TRAIL receptor mAb therapy to human glioma, providing a basis for further testing of its efficacy using spontaneous glioma models or in nonhuman primates. The administration of therapeutic mAbs to intraparenchymal neoplastic lesions in the brain might be limited by antibody penetration into the tumor. Macromolecules such as mAbs can, however, cross the blood–brain barrier (BBB) in clinically relevant concentrations in tumors with contrast enhancement, as seen in high-grade gliomas, which is indicative of having a disturbed BBB. Likewise, systemic administration of an mAb specific to EGFR was shown to effectively target and eradicate the established gliomas overexpressing EGFR in the nude mouse brain.[64] Another strategy to localize mAbs in the glioma, especially in the region of tumor cell infiltration where BBB is assumed intact, could be obtained by convection-enhanced delivery (CED). Saito *et al*[65] have shown that CED of sTRAIL resulted in the enhanced survival of mice bearing glioma in the brain in combination with temozolomide. Administration of pseudomonas end toxin conjugated to IL-13 (cintredekin besudotox) to patients with glioma by CED has already been tested under clinical trials.[66] Furthermore, combining mAb therapy with other therapeutic modalities such as chemotherapy, radiotherapy, molecular-targeted therapy, or toxins has been shown to be more effective than antibody alone.[67–69] Indeed, combination of the anti-DR5 mAbs with cisplatin or HDAC inhibitors synergistically enhanced the cytotoxic effects in human glioma cells (unpublished observations; Frew et al.[53]) and will be further investigated to potentially overcome resistance to anti-DR5 mAb therapy.

Acknowledgments

The authors thank Dr J. Tschopp for a gift of c-FLIP constructs and S. Matsushima for technical assistance on flow cytometry.

Conflict of interest statement: None declared.

Funding

This work was supported in part by grants from the Ministry of Education, Culture, Sports, Science and Technology of Japan (17591529 to M.N.).

References

1. The committee of Brain Tumor Registry of Japan. Report of brain tumor registry of Japan (1969–1996). *Neurol Med Chir (Tokyo)*. 2003;43(suppl):34–96.

2. Stupp R, Mason WP, van den Bent MJ, et al. Radiotherapy plus concomitant and adjuvant temozolomide for glioblastoma. *N Engl J Med*. 2005;352:987–996.

3. Guchelaar HJ, Vermes A, Vermes I, Haanen C. Apoptosis: molecular mechanisms and implications for cancer chemotherapy. *Pharm World Sci.* 1997;19:119–125.
4. Ashkenazi A. Targeting death and decoy receptors of the tumour-necrosis factor superfamily. *Nat Rev Cancer.* 2002;2:420–430.
5. Pan G, O'Rourke K, Chinnaiyan AM, et al. The receptor for the cytotoxic ligand TRAIL. *Science.* 1997; 276:111–113.
6. Pan G, Ni J, Wei YF, Yu G, Gentz R, Dixit VM. An antagonist decoy receptor and a death domain-containing receptor for TRAIL [see comments]. *Science.* 1997;277:815–818.
7. Sheridan JP, Marsters SA, Pitti RM, et al. Control of TRAIL-induced apoptosis by a family of signaling and decoy receptors [see comments]. *Science.* 1997;277:818–821..
8. Ashkenazi A, Pai RC, Fong S, et al. Safety and antitumor activity of recombinant soluble Apo2 ligand. *J Clin Invest.* 1999;104:155–162.
9. Nagane M, Pan G, Weddle JJ, Dixit VM, Cavenee WK, Huang HJ. Increased death receptor 5 expression by chemotherapeutic agents in human gliomas causes synergistic cytotoxicity with tumor necrosis factor-related apoptosis-inducing ligand in vitro and in vivo. *Cancer Res.* 2000;60:847–853.
10. Pitti RM, Marsters SA, Ruppert S, Donahue CJ, Moore A, Ashkenazi A. Induction of apoptosis by Apo-2 ligand, a new member of the tumor necrosis factor cytokine family. *J Biol Chem.* 1996;271:12687–12690.
11. Rieger J, Naumann U, Glaser T, Ashkenazi A, Weller M. APO2 ligand: a novel lethal weapon against malignant glioma? *FEBS Lett.* 1998; 427:124–128.
12. Wiley SR, Schooley K, Smolak PJ, et al. Identification and characterization of a new member of the TNF family that induces apoptosis. *Immunity.* 1995;3:673–682.
13. Song JH, Bellail A, Tse MC, Yong VW, Hao C. Human astrocytes are resistant to Fas ligand and tumor necrosis factor-related apoptosis-inducing ligand-induced apoptosis. *J Neurosci.* 2006;26:3299–3308.
14. Johnstone RW, Frew AJ, Smyth MJ. The TRAIL apoptotic pathway in cancer onset, progression and therapy. *Nat Rev Cancer.* 2008;8:782–798.
15. Degli-Esposti MA, Dougall WC, Smolak PJ, Waugh JY, Smith CA, Goodwin RG. The novel receptor TRAIL-R4 induces NF-kappaB and protects against TRAIL-mediated apoptosis, yet retains an incomplete death domain. *Immunity.* 1997;7:813–820.
16. Marsters SA, Sheridan JP, Pitti RM, et al. A novel receptor for Apo2 L/TRAIL contains a truncated death domain. *Curr Biol.* 1997;7:1003–1006.
17. Emery JG, McDonnell P, Burke MB, et al. Osteoprotegerin is a receptor for the cytotoxic ligand TRAIL. *J Biol Chem.* 1998;273:14363–14367.
18. Frank S, Köhler U, Schackert G, Schackert HK. Expression of TRAIL and its receptors in human brain tumors. *Biochem Biophys Res Commun.* 1999;257:454–459.
19. Almasan A, Ashkenazi A. Apo2 L/TRAIL: apoptosis signaling, biology, and potential for cancer therapy. *Cytokine Growth Factor Rev.* 2003;14:337–348.
20. Green DR, Reed JC. Mitochondria and apoptosis. *Science.* 1998;281:1309–1312.
21. Younes A, Kadin ME. Emerging applications of the tumor necrosis factor family of ligands and receptors in cancer therapy. *J Clin Oncol.* 2003;21:3526–3534.
22. Xiao C, Yang BF, Asadi N, Beguinot F, Hao C. Tumor necrosis factor-related apoptosis-inducing ligand-induced death-inducing signaling complex and its modulation by c-FLIP and PED/PEA-15 in glioma cells. *J Biol Chem.* 2002;277:25020–25025.
23. Vogler M, Durr K, Jovanovic M, Debatin KM, Fulda S. Regulation of TRAIL-induced apoptosis by XIAP in pancreatic carcinoma cells. *Oncogene.* 2007;26:248–257.
24. Khanbolooki S, Nawrocki ST, Arumugam T, et al. Nuclear factor-kappaB maintains TRAIL resistance in human pancreatic cancer cells. *Mol Cancer Ther.* 2006;5:2251–2260.
25. Cheng J, Hylander BL, Baer MR, Chen X, Repasky EA. Multiple mechanisms underlie resistance of leukemia cells to Apo2 Ligand/TRAIL. *Mol Cancer Ther.* 2006;5:1844–1853.
26. Yang LQ, Fang DC, Wang RQ, Yang SM. Effect of NF-kappaB, survivin, Bcl-2 and Caspase3 on apoptosis of gastric cancer cells induced by tumor necrosis factor related apoptosis inducing ligand. *World J Gastroenterol.* 2004;10:22–25.
27. Zhang XD, Borrow JM, Zhang XY, Nguyen T, Hersey P. Activation of ERK1/2 protects melanoma cells from TRAIL-induced apoptosis by inhibiting Smac/DIABLO release from mitochondria. *Oncogene.* 2003;22:2869–2881.
28. Chawla-Sarkar M, Bae SI, Reu FJ, Jacobs BS, Lindner DJ, Borden EC. Downregulation of Bcl-2, FLIP or IAPs (XIAP and survivin) by siRNAs sensitizes resistant melanoma cells to Apo2 L/TRAIL-induced apoptosis. *Cell Death Differ.* 2004;11:915–923.
29. Fulda S, Meyer E, Debatin KM. Inhibition of TRAIL-induced apoptosis by Bcl-2 overexpression. *Oncogene.* 2002;21:2283–2294.
30. Kandasamy K, Srivastava RK. Role of the phosphatidylinositol 3'-kinase/PTEN/Akt kinase pathway in tumor necrosis factor-related apoptosis-inducing ligand-induced apoptosis in non-small cell lung cancer cells. *Cancer Res.* 2002;62:4929–4937.
31. Hopkins-Donaldson S, Bodmer JL, Bourloud KB, Brognara CB, Tschopp J, Gross N. Loss of caspase-8 expression in neuroblastoma is related to malignancy and resistance to TRAIL-induced apoptosis. *Med Pediatr Oncol.* 2000;35:608–611.
32. Nagane M, Cavenee WK, Shiokawa Y. Synergistic cytotoxicity through the activation of multiple apoptosis pathways in human glioma cells induced by combined treatment with ionizing radiation and tumor necrosis factor-related apoptosis-inducing ligand. *J Neurosurg.* 2007;106:407–416.
33. Walczak H, Miller RE, Ariail K, et al. Tumoricidal activity of tumor necrosis factor-related apoptosis-inducing ligand in vivo [see comments]. *Nat Med.* 1999;5:157–163.
34. Lawrence D, Shahrokh Z, Marsters S, et al. Differential hepatocyte toxicity of recombinant Apo2 L/TRAIL versions. *Nat Med.* 2001;7:383–385.
35. Qin J, Chaturvedi V, Bonish B, Nickoloff BJ. Avoiding premature apoptosis of normal epidermal cells. *Nat Med.* 2001;7:385–386.
36. Gajewski TF. On the TRAIL toward death receptor-based cancer therapeutics. *J Clin Oncol.* 2007;25:1305–1307.
37. Ichikawa K, Liu W, Zhao L, et al. Tumoricidal activity of a novel anti-human DR5 monoclonal antibody without hepatocyte cytotoxicity. *Nat Med.* 2001;7:954–960.
38. Mori E, Thomas M, Motoki K, et al. Human normal hepatocytes are susceptible to apoptosis signal mediated by both TRAIL-R1 and TRAIL-R2. *Cell Death Differ.* 2004;11:203–207.
39. Motoki K, Mori E, Matsumoto A, et al. Enhanced apoptosis and tumor regression induced by a direct agonist antibody to tumor necrosis factor-related apoptosis-inducing ligand receptor 2. *Clin Cancer Res.* 2005;11:3126–3135.
40. Nagane M, Coufal F, Lin H, Bögler O, Cavenee WK, Huang HJS. A common mutant epidermal growth factor receptor confers enhanced tumorigenicity on human glioblastoma cells by increasing proliferation and reducing apoptosis. *Cancer Res.* 1996;56:5079–5086.

41. Nagane M, Narita Y, Mishima K, et al. Human glioblastoma xenografts overexpressing a tumor-specific mutant epidermal growth factor receptor sensitized to cisplatin by the AG1478 tyrosine kinase inhibitor. *J Neurosurg.* 2001;95:472–479.
42. Chuntharapai A, Dodge K, Grimmer K, et al. Isotype-dependent inhibition of tumor growth in vivo by monoclonal antibodies to death receptor 4. *J Immunol.* 2001;166:4891–4898.
43. Xu Y, Szalai AJ, Zhou T, et al. Fc gamma Rs modulate cytotoxicity of anti-Fas antibodies: implications for agonistic antibody-based therapeutics. *J Immunol.* 2003;171:562–568.
44. Kaufmann SH, Earnshaw WC. Induction of apoptosis by cancer chemotherapy. *Exp Cell Res.* 2000;256:42–49.
45. Zheng SJ, Wang P, Tsabary G, Chen YH. Critical roles of TRAIL in hepatic cell death and hepatic inflammation. *J Clin Invest.* 2004;113:58–64.
46. Georgakis GV, Li Y, Humphreys R, et al. Activity of selective fully human agonistic antibodies to the TRAIL death receptors TRAIL-R1 and TRAIL-R2 in primary and cultured lymphoma cells: induction of apoptosis and enhancement of doxorubicin- and bortezomib-induced cell death. *Br J Haematol.* 2005;130:501–510.
47. Pukac L, Kanakaraj P, Humphreys R, et al. HGS-ETR1, a fully human TRAIL-receptor 1 monoclonal antibody, induces cell death in multiple tumour types in vitro and in vivo. *Br J Cancer.* 2005;92:1430–1441.
48. Takeda K, Yamaguchi N, Akiba H, et al. Induction of tumor-specific T cell immunity by anti-DR5 antibody therapy. *J Exp Med.* 2004;199:437–448.
49. Nagane M, Asai A, Shibui S, Nomura K, Matsutani M, Kuchino Y. Expression of O^6-methylguanine-DNA methyltransferase and chloroethylnitrosourea resistance of human brain tumors. *Jpn J Clin Oncol.* 1992;22:143–149.
50. Hotte SJ, Hirte HW, Chen EX, et al. A phase 1 study of mapatumumab (fully human monoclonal antibody to TRAIL-R1) in patients with advanced solid malignancies. *Clin Cancer Res.* 2008;14:3450–3455.
51. Plummer R, Attard G, Pacey S, et al. Phase 1 and pharmacokinetic study of lexatumumab in patients with advanced cancers. *Clin Cancer Res.* 2007;13:6187–6194.
52. Tolcher AW, Mita M, Meropol NJ, et al. Phase I pharmacokinetic and biologic correlative study of mapatumumab, a fully human monoclonal antibody with agonist activity to tumor necrosis factor-related apoptosis-inducing ligand receptor-1. *J Clin Oncol.* 2007;25:1390–1395.
53. Frew AJ, Lindemann RK, Martin BP, et al. Combination therapy of established cancer using a histone deacetylase inhibitor and a TRAIL receptor agonist. *Proc Natl Acad Sci USA.* 2008;105:11317–11322.
54. Kelley RF, Totpal K, Lindstrom SH, et al. Receptor-selective mutants of apoptosis-inducing ligand 2/tumor necrosis factor-related apoptosis-inducing ligand reveal a greater contribution of death receptor (DR) 5 than DR4 to apoptosis signaling. *J Biol Chem.* 2005;280:2205–2212.
55. Rohn TA, Wagenknecht B, Roth W, et al. CCNU-dependent potentiation of TRAIL/Apo2 L-induced apoptosis in human glioma cells is p53-independent but may involve enhanced cytochrome c release. *Oncogene.* 2001;20:4128–4137.
56. Irmler M, Thome M, Hahne M, et al. Inhibition of death receptor signals by cellular FLIP [see comments]. *Nature.* 1997;388:190–195.
57. Krueger A, Schmitz I, Baumann S, Krammer PH, Kirchhoff S. Cellular FLICE-inhibitory protein splice variants inhibit different steps of caspase-8 activation at the CD95 death-inducing signaling complex. *J Biol Chem.* 2001;276:20633–20640.
58. Kataoka T. The caspase-8 modulator c-FLIP. *Crit Rev Immunol.* 2005;25:31–58.
59. Ricci MS, Jin Z, Dews M, et al. Direct repression of FLIP expression by c-myc is a major determinant of TRAIL sensitivity. *Mol Cell Biol.* 2004;24:8541–8555.
60. Yang BF, Xiao C, Roa WH, Krammer PH, Hao C. Calcium/calmodulin-dependent protein kinase II regulation of c-FLIP expression and phosphorylation in modulation of Fas-mediated signaling in malignant glioma cells. *J Biol Chem.* 2003;278:7043–7050.
61. Rieger J, Frank B, Weller M, Wick W. Mechanisms of resistance of human glioma cells to Apo2 ligand/TNF-related apoptosis-inducing ligand. *Cell Physiol Biochem.* 2007;20:23–34.
62. Panner A, James CD, Berger MS, Pieper RO. mTOR controls FLIPs translation and TRAIL sensitivity in glioblastoma multiforme cells. *Mol Cell Biol.* 2005;25:8809–8823.
63. Zhou Q, Fukushima P, DeGraff W, et al. Radiation and the Apo2 L/TRAIL apoptotic pathway preferentially inhibit the colonization of premalignant human breast cells overexpressing cyclin D1. *Cancer Res.* 2000;60:2611–2615.
64. Mishima K, Johns TG, Luwor RB, et al. Growth suppression of intracranial xenografted glioblastomas overexpressing mutant epidermal growth factor receptors by systemic administration of monoclonal antibody (mAb) 806, a novel monoclonal antibody directed to the receptor. *Cancer Res.* 2001;61:5349–5354.
65. Saito R, Bringas JR, Panner A, et al. Convection-enhanced delivery of tumor necrosis factor-related apoptosis-inducing ligand with systemic administration of temozolomide prolongs survival in an intracranial glioblastoma xenograft model. *Cancer Res.* 2004;64:6858–6862.
66. Vogelbaum MA, Sampson JH, Kunwar S, et al. Convection-enhanced delivery of cintredekin besudotox (interleukin-13-PE38QQR) followed by radiation therapy with and without temozolomide in newly diagnosed malignant gliomas: phase 1 study of final safety results. *Neurosurgery.* 2007;61:1031–1037; discussion 1037–1038.
67. Green MC, Murray JL, Hortobagyi GN. Monoclonal antibody therapy for solid tumors. *Cancer Treat Rev.* 2000;26:269–286.
68. Trail PA, Bianchi AB. Monoclonal antibody drug conjugates in the treatment of cancer. *Curr Opin Immunol.* 1999;11:584–588.
69. Pietras RJ, Pegram MD, Finn RS, Maneval DA, Slamon DJ. Remission of human breast cancer xenografts on therapy with humanized monoclonal antibody to HER-2 receptor and DNA-reactive drugs. *Oncogene.* 1998;17:2235–2249.

SHP-2/*PTPN11* mediates gliomagenesis driven by *PDGFRA* and *INK4A/ARF* aberrations in mice and humans

Kun-Wei Liu,[1,2] Haizhong Feng,[1,2] Robert Bachoo,[3] Andrius Kazlauskas,[4] Erin M. Smith,[5] Karen Symes,[5] Ronald L. Hamilton,[2] Motoo Nagane,[6] Ryo Nishikawa,[7] Bo Hu,[1,8] and Shi-Yuan Cheng[1,2]

[1]University of Pittsburgh Cancer Institute and [2]Department of Pathology, University of Pittsburgh School of Medicine, Pittsburgh, Pennsylvania, USA. [3]Department of Internal Medicine, University of Texas Southwestern Medical Center, Dallas, Texas, USA. [4]Schepens Eye Research Institute and Harvard Medical School, Boston, Massachusetts, USA. [5]Department of Biochemistry, Boston University School of Medicine, Boston, Massachusetts, USA. [6]Department of Neurosurgery, Kyorin University Faculty of Medicine, Tokyo, Japan. [7]Department of Neurosurgery, Saitama Medical University, Saitama-ken, Japan. [8]Department of Medicine, University of Pittsburgh School of Medicine, Pittsburgh, Pennsylvania, USA.

Recent collaborative efforts have subclassified malignant glioblastomas into 4 clinical relevant subtypes based on their signature genetic lesions. Platelet-derived growth factor receptor α (*PDGFRA*) overexpression is concomitant with a loss of cyclin-dependent kinase inhibitor 2A (*CDKN2A*) locus (encoding P16INK4A and P14ARF) in a large number of tumors within one subtype of glioblastomas. Here we report that activation of PDGFRα conferred tumorigenicity to *Ink4a/Arf*-deficient mouse astrocytes and human glioma cells in the brain. Restoration of p16INK4a but not p19ARF suppressed PDGFRα-promoted glioma formation. Mechanistically, abrogation of signaling modules in PDGFRα that lost capacity to bind to SHP-2 or PI3K significantly diminished PDGFRα-promoted tumorigenesis. Furthermore, inhibition of SHP-2 by shRNAs or pharmacological inhibitors disrupted the interaction of PI3K with PDGFRα, suppressed downstream AKT/mTOR activation, and impaired tumorigenesis of *Ink4a/Arf*-null cells, whereas expression of an activated PI3K mutant rescued the effect of SHP-2 inhibition on tumorigenicity. PDGFRα and PDGF-A are co-expressed in clinical glioblastoma specimens, and such co-expression is linked with activation of SHP-2/AKT/mTOR signaling. Together, our data suggest that in glioblastomas with *Ink4a/Arf* deficiency, overexpressed PDGFRα promotes tumorigenesis through the PI3K/AKT/mTOR-mediated pathway regulated by SHP-2 activity. These findings functionally validate the genomic analysis of glioblastomas and identify SHP-2 as a potential target for treatment of glioblastomas.

Introduction

Human gliomas account for the most common and malignant tumors in the CNS (1). Despite intensive treatments including maximal surgical resection, combined with radiotherapy and concurrent or adjuvant chemotherapies, median survival time of patients with high-grade glioblastoma multiforme (GBM) remains 14–16 months after diagnosis (1, 2). Recently, coordinated genomic analyses of a large cohort of clinical GBM specimens identified frequent co-alterations of genes in 3 core pathways — the P53, retinoblastoma (RB), and receptor tyrosine kinase (RTK) pathways — that are crucial in gliomagenesis (3). Notably, the gene encoding platelet-derived growth factor receptor α (PDGFRα) is amplified in approximately 13% of total GBMs analyzed, and deletion of the tumor suppressor cyclin-dependent kinase inhibitor 2A (*CDKN2A*) locus is frequently found in these PDGFRα-amplified GBMs (3, 4). However, to our knowledge, studies have not been conducted to determine whether these genetic aberrations act in concert to promote gliomagenesis, or to determine the underlying mechanisms of PDGFRα-stimulated tumorigenesis.

The homozygous deletion of the *CDKN2A* locus at chromosome 9p21, which eliminates both *INK4A* and *ARF* genes (encoding P16INK4A and P14ARF, respectively), concomitantly deregulates 2 of the major tumor suppressor pathways, the RB and P53 pathways (5). Mice lacking the *Cdkn2a* locus develop spontaneous tumors and are more prone to carcinogenesis (6). Whereas no spontaneous tumors are found in the brain of *Ink4a/Arf*-deficient mice, astrocytes and neural stem cells (NSCs) from these mice form high-grade gliomas in the brain upon EGFR activation (7). Additionally, K-Ras activation has been shown to cooperate with loss of *Ink4a* and *Arf* in mouse astrocytes (mAsts) or neural progenitor cells to generate GBMs (8).

PDGFRα is a RTK that elicits a variety of biological activities such as cell proliferation and migration via stimulation by its ligand dimers, PDGF-AA, -AB, -BB, -CC, and -DD. Activated PDGFRα associates via the autophosphorylated tyrosine (p-Y) residues at its cytoplasmic domain to various downstream SH2 domain–containing signaling molecules, including SRC family kinases (SFKs), phosphotyrosine phosphatase SHP-2, PI3K, and PLCγ (9, 10). Mice deficient in PDGFRα or PDGF-A or engineered to separately express PDGFRα with mutations of the individual p-Y sites show alterations in cellular behavior and embryo development (9, 11). In particular, PI3K has been identified as the major effector of PDGFRα signaling in vitro and in vivo (10, 12, 13). SFKs and PLCγ contribute to some but not all PDGFRα functions (10, 12–14), whereas SHP-2 is not required for cell survival during Xenopus embryogenesis (12). However, contributions of each of these signaling modules to glioma formation have not to our knowledge been demonstrated.

Conflict of interest: The authors have declared that no conflict of interest exists.

Citation for this article: *J Clin Invest.* 2011;121(3):905–917. doi:10.1172/JCI43690.

Activation of PDGFRα signaling has been observed in human gliomas. In clinical glioma specimens, PDGFRα and PDGF-A are overexpressed in tumor cells, while PDGFRβ is only expressed in endothelial and peri-endothelial compartments (15). PDGF-B, which binds to both PDGFRα and PDGFRβ, is an oncoprotein that causes glioma formation in the brain (16). Loss of *Ink4a/Arf* in mAsts enhances PDGF-B–initiated gliomagenesis and tumor progression in the brain (16). Specific activation of PDGFRα signaling by infusion of PDGF-A proteins, which only bind to PDGFRα in PDGFRα-positive type B NSCs in the subventricular zone (SVZ), leads to glioma-like growth of these cells in adult brain (17). However, how the activation of PDGFRα signaling causes glioma formation and whether co-alteration of tumor suppressor pathways is required in PDGFRα-mediated gliomagenesis have not been directly shown. In this study, we determined the synergistic impact of *PDGFRA* overexpression and *INK4A/ARF* deletion on gliomagenesis in mAsts and human glioma cells. We then used genetic and pharmacological approaches targeting individual downstream signaling enzymes to examine which specific signaling pathway(s) emanating from PDGFRα are critical in tumorigenesis. Furthermore, we confirmed our observations in clinical glioma specimens that co-overexpress PDGFRα and PDGF-A.

Results

Overexpression of PDGFRα and/or PDGF-A confers tumorigenicity to Ink4a/Arf$^{-/-}$ mAsts. To determine whether activation of PDGFRα signaling in *Ink4a/Arf$^{-/-}$* mAsts leads to gliomagenesis in the brain, we overexpressed PDGFRα and/or its ligand PDGF-A chain in a retroviral vector containing an IRES-GFP in *Ink4a/Arf$^{-/-}$* mAsts (Figure 1A). The impact of PDGFRα/PDGF-A overexpression on the growth and survival of these cells in vitro was moderate (Supplemental Figure 1, A and B; supplemental material available online with this article; doi:10.1172/JCI43690DS1). However, when these cells were separately transplanted into the flanks of mice, significant s.c. tumor growth was evident in mice that separately received *Ink4a/Arf$^{-/-}$* mAsts expressing PDGFRα, PDGF-A, or PDGFRα/PDGF-A (with the receptor and ligand co-expressed in the same cell to create an autocrine signaling), whereas minimal or no tumor formation was seen in control mice that received *Ink4a/Arf$^{-/-}$* mAsts expressing GFP (Figure 1B). To determine tumorigenicity of these cells in the brain, various mAsts were separately implanted into the brain of mice. Notably, mice that received GFP mAsts did not show active tumor growth up to 42 days after implantation, while PDGFRα, PDGF-A, and PDGFRα/PDGF-A mAsts started to form tumors in the brain as early as 8–11 days and the majority of tumors reached a volume of approximately 25 to 30 mm^3 in 25–35 days. Moreover, mice that separately received PDGFRα- or PDGF-A–expressing mAsts survived up to 2 months after implantation. On the other hand, all mice that received autocrine PDGFRα/PDGF-A–expressing mAsts developed large and invasive tumors by 20 days, with an average survival time of 25 days after implantation. As shown in Figure 1, C–L, significantly larger and highly invasive gliomas formed in the brains of mice that received *Ink4a/Arf$^{-/-}$* mAsts overexpressing PDGFRα, PDGF-A, or PDGFRα/PDGF-A, whereas only small tumor lesions were found in the brain of mice that received control mAsts. Significantly, an approximately 10-fold increase in the cell proliferation index was found in gliomas derived from PDGFRα-activated mAsts compared with control tumors (Figure 1, M–R), whereas an approximately 10-fold decrease of cell apoptosis was seen in PDGFRα/PDGF-A–expressing tumors (Figure 1S). Of note, in established s.c. or brain tumors, exogenous expression of PDGFRα or PDGF-A was maintained at the end of the experiments (Supplemental Figure 1, C–K, and data not shown). Taken together, these results indicate that expression of PDGFRα and/or PDGF-A confers tumorigenicity to *Ink4a/Arf*-deficient mAsts in the brain.

To further characterize the tumors derived from *Ink4a/Arf$^{-/-}$* PDGFRα mAsts, we examined molecular markers of various cell lineages in the CNS development. As shown in Figure 2, tumors derived from PDGFRα-expressing mAsts were highly positive for the neural progenitor marker nestin, which was distributed along the processes of individual cells (Figure 2, A and B). As expected, most of tumor cells showed expression of the progenitor/mature astrocyte marker GFAP (Figure 2, C and D) but were negative for the neuronal marker class III β-tubulin (TUJ1) (Figure 2, E and F). Significantly, NG2, an oligodendrocyte progenitor cell marker (18), was expressed in a population of tumor cells that were actively invading the surrounding brain parenchyma, whereas the core of the tumor mass showed relatively low NG2 expression (Figure 2, G and H). In contrast, control tumors derived from *Ink4a/Arf$^{-/-}$* GFP mAsts lacked nestin or NG2 expression (data not shown). In addition, tumors derived from *Ink4a/Arf$^{-/-}$* PDGFRα mAsts showed negative staining for oligodendrocyte type 2 astrocyte progenitor marker A2B5 and an oligodendrocyte marker CNPase (data not shown). Notably, brain tumors derived from *Ink4a/Arf$^{-/-}$* PDGFRα/PDGF-A mAsts (data not shown) displayed similar IHC features to tumors derived from *Ink4a/Arf$^{-/-}$* PDGFRα mAsts, suggesting that similar dedifferentiation events also occurred in autocrine PDGFRα/PDGF-A–co-expressing tumors.

Exogenous expression of PDGF-A enhances tumorigenicity of Ink4a/Arf-null but not WT Ink4a/Arf human glioma cells in the brain. Next, we used 4 human glioma cell lines that were either *INK4A/ARF* null (LN444 and LN443) or WT *INK4A/ARF* (LN-Z308 and LN319; Figure 3A) (19) and exogenously expressed PDGF-A in these glioma cells that express endogenous PDGFRα (Figure 3B). In vitro, expression of PDGF-A in *INK4A/ARF*-null LN444 cells significantly enhanced their capacity of anchorage-independent growth in soft agar, whereas a minimal effect was seen in WT *INK4A/ARF* LN-Z308 and LN319 cells (Figure 3C). When various glioma cells were separately implanted into the brain or the flanks of mice, PDGF-A expression markedly enhanced tumor growth and invasion of *INK4A/ARF*-null LN444 and LN443 glioma cells, while minimal impact of PDGF-A expression on tumorigenesis or invasion was seen in WT *INK4A/ARF* LN-Z308 and LN319 cells in both anatomic sites (Figure 3, D–K, and Supplemental Figure 2). Mice received LN444/PDGF-A cells in the brain had tumor onset as early as 35 days, while mice with LN443/PDGF-A cells developed invasive intracranial tumor 25–30 days after implantation. In contrast, LN444 and LN443 parental cells only formed small tumor lesions in the brain up to 2–3 months following implantation. Mice that received LN444/PDGF-A cells survived for 75–80 days, while most of the mice that received LN443/PDGF-A cells lived up to 3 months after implantation. On the other hand, no significant brain tumor growth was found 2–3 months after implantation in mice that received LN-Z308/PDGF-A or LN319/PDGF-A cells. Thus, consistent with our findings in the *Ink4a/Arf$^{-/-}$* mAsts, these data indicate that PDGFRα/PDGF-A signaling enhances in vivo tumor growth and invasion of human glioma cells deficient in *INK4A/ARF*.

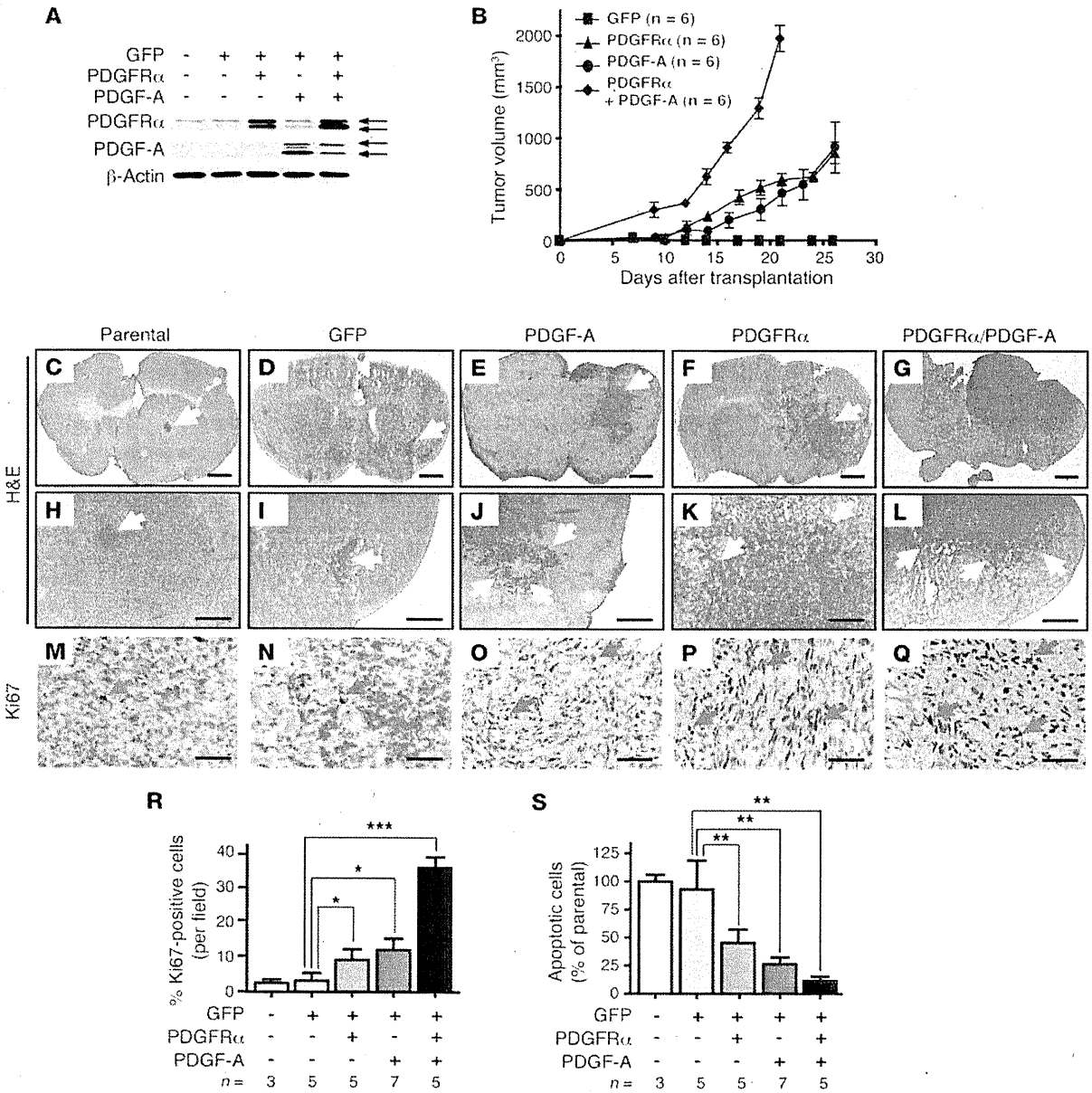

Figure 1

PDGFRα and/or PDGF-A overexpression promotes tumorigenesis of *Ink4a/Arf*$^{-/-}$ mAsts. (**A**) IB analysis of exogenous expression of PDGFRα and/or PDGF-A in mAsts. Arrows indicate PDGFRα and PDGF-A proteins run as doublet bands. β-Actin was used as a loading control. (**B**) Tumor growth of various mAsts s.c. Data are shown as mean ± SD. (**C–L**) Representative H&E staining images of various brain sections from 2 independent experiments with at least 3–5 mice per group with similar results. Brains were harvested 25–30 days after transplantation for **C–F** and 20 days after transplantation for **G**. Scale bars: 1 mm (**C–G**); 200 μm (**H–L**). (**M–Q**) Ki-67 staining of the corresponding brain sections in (**C–G**). Yellow arrows indicate tumor mass or invading tumor cells. Red arrows indicate Ki-67–positive cells. Scale bars: 50 μm. (**R** and **S**) Quantification of Ki-67 staining (**R**) and TUNEL staining (**S**) of various brain sections. Data are presented as percentage to parental controls (mean ± SD). *n*, the number of mice used for each group. **P* < 0.05; ***P* < 0.01; ****P* < 0.001.

p16INK4a but not p19ARF attenuates the PDGFRα-promoted tumorigenesis of Ink4a/Arf-deficient mAsts and human glioma cells. To investigate whether re-expression p16INK4a or p19ARF is able to abrogate the enhanced tumorigenicity in *Ink4a/Arf*$^{-/-}$ mAsts, we separately expressed these 2 tumor suppressors in mAsts (Figure 4A). Surprisingly, re-expression of p16INK4a but not p19ARF alone in *Ink4a/Arf*$^{-/-}$ mAsts suppressed soft agar growth of PDGFRα-expressing mAsts stimulated by PDGF-A (Figure 4B). Consistently, enforced restoration of p16INK4a in *Ink4a/Arf*$^{-/-}$ mAsts significantly inhibited tumorigenesis of PDGFRα/PDGF-A–overexpressing mAsts in the mouse brain (Figure 4C). To further demonstrate the cooperative effect of PDGFRα activation and loss of *Ink4a* on tumorigenesis, we knocked down endogenous p16INK4a using shRNAs targeting *CDKN2A* in

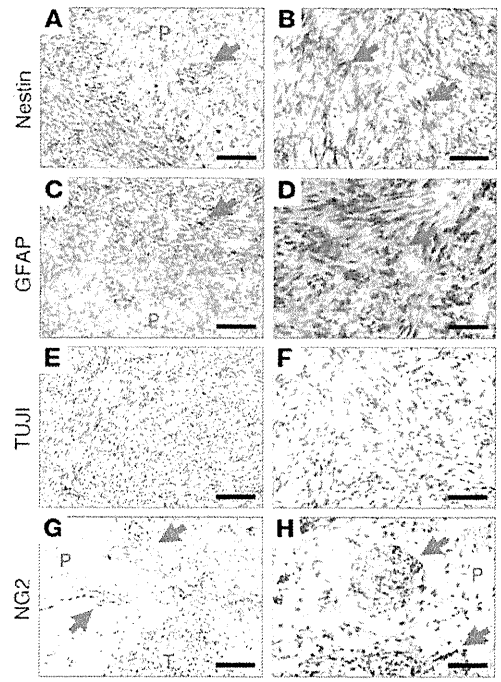

Figure 2
Tumors derived from *Ink4a/Arf*$^{-/-}$ PDGFRα mAsts express markers of neural progenitor cells. Representative images of IHC staining using antibodies against nestin (**A** and **B**), GFAP (**C** and **D**), βIII-tubulin (**E** and **F**), and NG2 (**G** and **H**). Arrows indicate positive staining of various markers. T, tumor mass; P, normal brain parenchyma. Scale bars: 100 μm (**A**, **C**, **E**, and **G**); 50 μm (**B**, **D**, **F**, and **H**).

WT *INK4A/ARF* LN319 cells. As shown in Figure 4D, significant inhibition of P16INK4A without affecting P14ARF expression by 2 separate shRNAs in LN319 cells resulted in a marked increase in colony formation in soft agar. Since p16INK4a inhibits CDK4/6, which inactivates RB by phosphorylation, and since p19ARF (or P14ARF) targets MDM2, which suppresses p53 (5), we thus examined responses of modulating CDK4/6 and p53 in these cells. As shown in Figure 4E, inhibition of phosphorylation of RB, the direct downstream target of CDK4/6 by CDK4/6 inhibitor PD0332991 (20), markedly reduced PDGF-A–stimulated cell growth of *Ink4a/Arf*-deficient mAsts and LN444 cells in soft agar, which suggests that the tumorigenic effect of PDGFRα signaling is dependent on CDK4/6 inactivation of RB proteins (p-RB). Since we did not observe any tumor-suppressing effect of p19ARF on *Ink4a/Arf*$^{-/-}$ PDGFRα-expressing mAsts (Figure 4B), we asked whether the downstream p53 protein was functional in these cells. When *Ink4a/Arf*$^{-/-}$ and *Ink4a/Arf*$^{-/-}$ p19ARF mAsts were treated with cisplatin (21), p53 expression was strongly induced in *Ink4a/Arf*$^{-/-}$ PDGFRα/p19ARF-expressing mAsts but only moderately induced in *Ink4a/Arf*$^{-/-}$ PDGFRα-expressing mAsts (Supplemental Figure 3A). The mAsts expressing p19ARF were more sensitive to cisplatin inhibition of cell survival than those without p19ARF expression, indicating that p19ARF-upregulated p53 in *Ink4a/Arf*$^{-/-}$ PDGFRα-expressing mAsts rendered sensitivity to cisplatin inhibition (Supplemental Figure 3B). Collectively, these data show that p16INK4a but not p19ARF suppresses the tumorigenesis promoted by PDGFRα/PDGF-A signaling, suggesting a cooperative effect of PDGFRα activation and p16INK4a inhibition during gliomagenesis. Additionally, p19ARF loss might be required for tumor survival in certain circumstances such as in the presence of DNA-damaging agents.

PDGFRα-enhanced tumorigenicity is mediated by SHP-2 and PI3K signaling. Previous studies using genetic and biochemical approaches have defined the roles of signaling molecules in PDGFRα-mediated cellular functions by specific tyrosine-to-phenylalanine (Y-to-F) mutations (Figure 5A) (10, 12, 13). To investigate the impact of these PDGFRα mutations on tumorigenesis, we separately expressed WT PDGFRα or various PDGFRα mutants in *Ink4a/Arf*$^{-/-}$ mAsts. The PDGFRα mutant R627 (PDGFRα-R627) that harbors a lysine-to-arginine (K-to-R) mutation was included as a "receptor kinase–dead" control. As shown in Figure 5B, stimulation of WT PDGFRα by PDGF-A resulted in autophosphorylation of the receptor and promoted phosphorylation of downstream signaling molecules Erk1/2 and Akt, whereas there was an undetectable receptor tyrosine autophosphorylation in PDGFRα-R627 (Figure 5B). PDGFRα Y-to-F mutations at Y572 and Y574 (PDGFRα-F572/74; for SFK binding), Y1018 (PDGFRα-F1018; for PLCγ binding), and Y988 (PDGFRα-F988) did not result in a significant decrease in p-Akt and p-Erk levels in response to PDGF-A stimulation (Figure 5B). Moreover, the mutation at Y731 and Y742 (PDGFRα-F731/42; for PI3K binding) led to a marked decrease in PDGF-A–stimulated p-Akt and p-Erk1/2 levels (Figure 5B). In agreement with a previous report (22), p-Erk1/2 was markedly reduced in PDGF-A–stimulated mAsts expressing PDGFRα-F720 (Y-to-F mutation at Y720; for SHP-2 binding), compared with WT PDGFRα mAsts (Figure 5B). Interestingly, p-Akt levels were also attenuated in PDGFRα-F720 cells.

Next, we determined the impact of these Y-to-F mutations on PDGFRα-promoted cell transformation of *Ink4a/Arf*$^{-/-}$ mAsts in vitro. As shown in Figure 5C, mAsts expressing WT PDGFRα and PDGFRα-F572/74, PDGFRα-F988, and PDGFRα-F1018 PDGFRα mutants showed similar capability of anchorage-independent growth in soft agar. In contrast, expression of PDGFRα-R627, PDGFRα-F731/42, or PDGFRα-F720 instead of WT PDGFRα significantly abrogated the capacity of mAsts to form colonies in soft agar (Figure 5, C and D), indicating that PI3K and SHP-2 signaling were critical for cell transformation in vitro. When various *Ink4a/Arf*$^{-/-}$ mAsts were separately implanted into the brains of mice, PDGFRα-R627, PDGFRα-F731/42, PDGFRα-F720, and PDGFRα-F988 significantly impaired PDGFRα-promoted tumorigenesis and invasion compared with WT PDGFRα (Figure 6, B, C, E, and F, compared with Figure 6A). However, mAsts expressing PDGFRα-F572/74 or PDGFRα-F1018 displayed tumorigenicity comparable to WT PDGFRα tumors (Figure 6, D and G, compared to 6A), but showed markedly reduced tumor invasion compared with the tumors derived from mAsts expressing WT PDGFRα (Figure 6, K and N, compared with 6H). Higher-magnification images of PDGFRα-R627, PDGFRα-F731/42, and PDGFRα-F720 mutants (Figure 6, I, J, and L) further illustrated that these mutations significantly negated the enhanced tumorigenicity conferred by PDGFRα activation, leading to the formation of tumors similar in volume and invasiveness to those seen in GFP-expressing mAst tumors (Figure 1, D and I). Moreover, PDGFRα-F731/42 and PDGFRα-F720 tumors showed a significantly decreased cell proliferation (Figure 6, O and P) and increased apoptosis

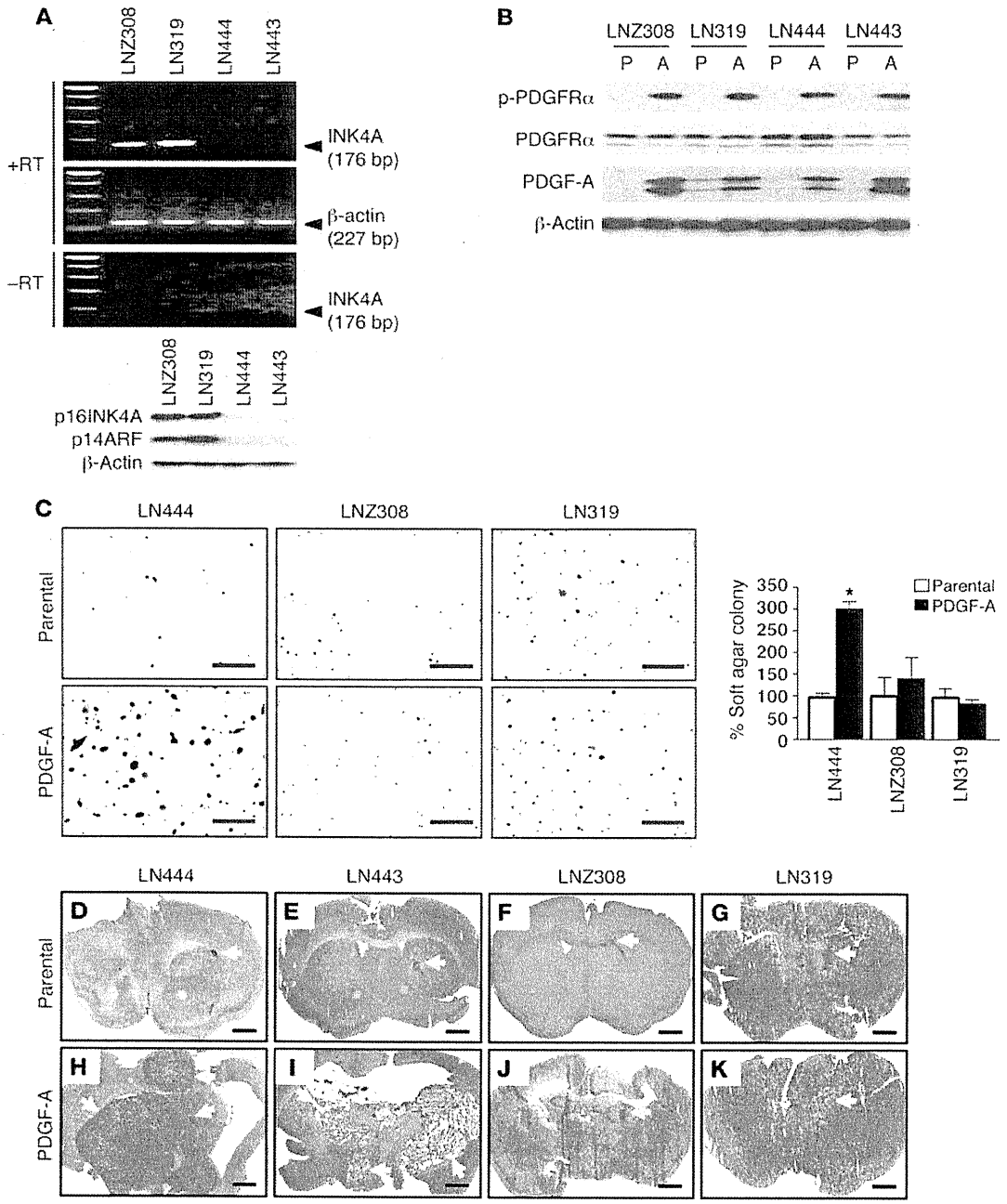

Figure 3

PDGF-A overexpression enhances tumorigenesis of *INK4A/ARF*-deficient but not WT *INK4A/ARF* human glioma cells. (**A**) RT-PCR (top) and IB analyses (bottom) of *INK4A/ARF*-deficient LN444 and LN443 and WT *INK4A/ARF* LN-Z308 and LN319 human glioma cells. (**B**) IB analysis of PDGF-A overexpression in glioma cells with endogenous PDGFRα expression. PDGFRα was phosphorylated at tyrosine residues in PDGF-A–expressing cells, but not in parental cells that have no detectable PDGF-A. P, parental cells; A, PDGF-A–overexpressing cells. β-Actin was used as a loading control in both **A** and **B**. (**C**) Representative images (left) and quantification (right) of anchorage-independent growth of various glioma cells in soft agar. Scale bars: 1 mm. Data are presented as percentage of the respective parental cells (mean ± SD). *$P < 0.001$, Student's *t* test. (**D**–**K**) Representative H&E-stained images of various brain sections from 2 independent experiments with 3–5 mice per group with similar results. Brains were harvested 50–55 days (**D** and **H**), 75–80 days (**E** and **I**), and 45–50 days (**F**, **G**, **J**, and **K**) after transplantation. Arrows indicate gliomas formed in the brain. Scale bar: 1 mm.

(Figure 6, Q and R), whereas PDGFRα-F572/74, PDGFRα-F988, and PDGFRα-F1018 tumors exhibited moderate or minimal impacts on cell proliferation and survival compared with WT PDGFRα tumors. Conversely, retention of any 1 of the 5 signaling modules (Y731/42, Y572/74, Y720, Y988, and Y1018 PDGFRα mutants) (10) was insufficient to rescue the abolished tumorigenesis in the brain (data not shown). Taken together, these data indicate that ablation of PDGFRα association with

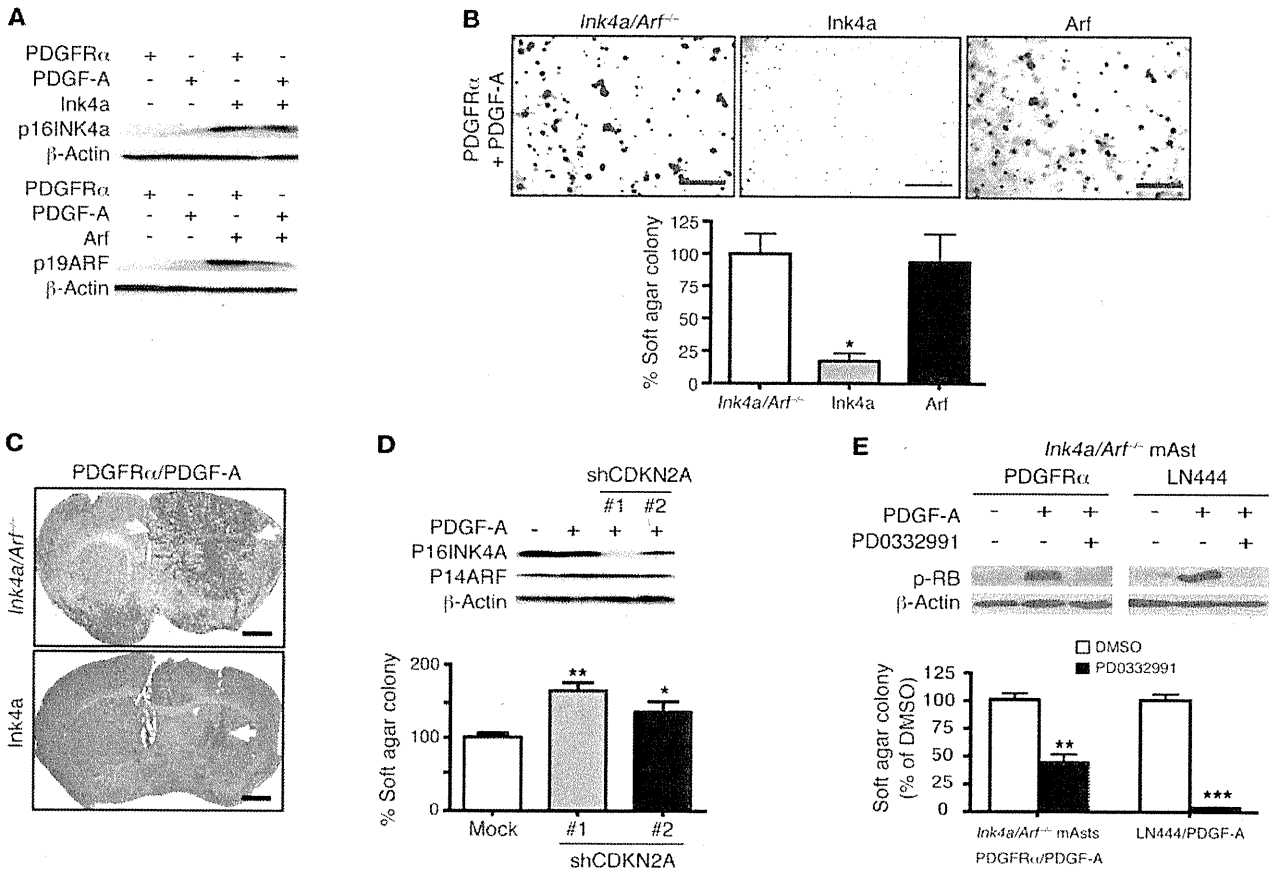

Figure 4

Re-expression of p16INK4a but not p19ARF suppresses the tumorigenesis of mAsts expressing PDGFRα/PDGF-A. (**A**) IB analyses of re-expression of p16INK4a or p19ARF in PDGFRα- or PDGF-A–overexpressing *Ink4a/Arf*$^{-/-}$ mAsts. (**B**) Top: Anchorage-independent growth of p16INK4a- or p19ARF-expressing mAsts. Scale bars: 1 mm. Bottom: Quantification of soft agar assays. Data are presented as mean ± SD. $^{*}P < 0.05$. (**C**) Representative H&E staining images of various brain sections from 2 independent experiments with 3–5 mice per group with similar results. Brains were harvested 18–22 days after implantation. Mice that received either type of cell displayed similar tumor onset and survival times as mice in Figure 1. Scale bars: 1 mm. (**D**) Anchorage-independent growth of WT *INK4A/ARF* LN319 cells transfected with shCDKN2A in soft agar. Top: IB analysis. Bottom: Quantification of soft agar assays. Two stable cell clones (#1 and #2) with different efficiencies of P16INK4A knockdown were used. Data are mean ± SD. (**E**) Soft agar growth of *Ink4a/Arf*-deficient mAsts and LN444 cells treated with PD0332991. Top: IB analysis. Bottom: Quantification of soft agar assays. β-Actin was used as a loading control in all IB experiments. Data are presented as mean ± SD and are representative of 2 independent experiments. $^{*}P < 0.05$; $^{**}P < 0.01$; $^{***}P < 0.001$.

SHP-2 or PI3K abrogates tumorigenicity of *Ink4a/Arf*$^{-/-}$ mAsts expressing PDGFRα, whereas individual association of PI3K, SHP-2, SFK, or PLCγ with the RTK was insufficient to elicit the full spectrum of tumor-promoting effects of PDGFRα.

Pharmacological inhibition of SHP-2 or PI3K abrogates PDGFRα-promoted tumorigenesis of Ink4a/Arf-deficient mAsts and human glioma cells. We further investigated whether inhibition of SHP-2 and PI3K activities by pharmacological approaches suppresses tumorigenicity of PDGFRα/PDGF-A–expressing *Ink4a/Arf*$^{-/-}$ mAst and LN444 cells. To this end, we exploited several pharmacological inhibitors against PI3K (LY294002), SHP-2 (PHPS-1 and NSC87877) (23), and SFKs (SU6656, and PP2). As shown in Figure 7, LY294002 inhibited PDGF-A–induced phosphorylation of Akt at 10 μM in mAsts and 5 μM in LN444 glioma cells, whereas Erk1/2 phosphorylation was unaffected by LY294002 treatment in both types of cells (Figure 7, A and B). Of note, a modest decrease was observed in p-Erk1/2 levels in mAsts treated with 20 μM LY294002 (Figure 7A). At a concentration of 100 μM (23), both PHPS-1 and NSC87877 significantly inhibited p-Erk1/2, a direct downstream target of SHP-2, in mAsts and LN444 cells (Figure 7, A and B). Next, we examined the impact of the pharmacological interventions of these signaling enzymes on in vitro cell transformation and found that 10 μM LY294002, which had no effect on Erk1/2 activation, suppressed soft agar growth of PDGFRα-expressing mAsts stimulated by PDGF-A (Figure 7A) and PDGF-A–expressing LN444 cells (Figure 7B). Similarly, 100 μM of either PHPS-1 or NSC87877 ablated PDGFRα-stimulated, anchorage-independent growth in soft agar but only had a minimal effect on the cell survival and caspase-3 activation of both PDGFRα/PDGF-A–expressing mAsts and LN444 cells in culture (Supplemental Figure 4, A and B). In contrast, 2 SFK inhibitors, SU6656 and PP2 each at 5-μM concentration, only showed a modest impact on tumorigenesis of these cells (Figure 7, A and B). Additionally, the MEK inhibitor PD98059 at 10 μM, which suppressed PDGF-A–induced

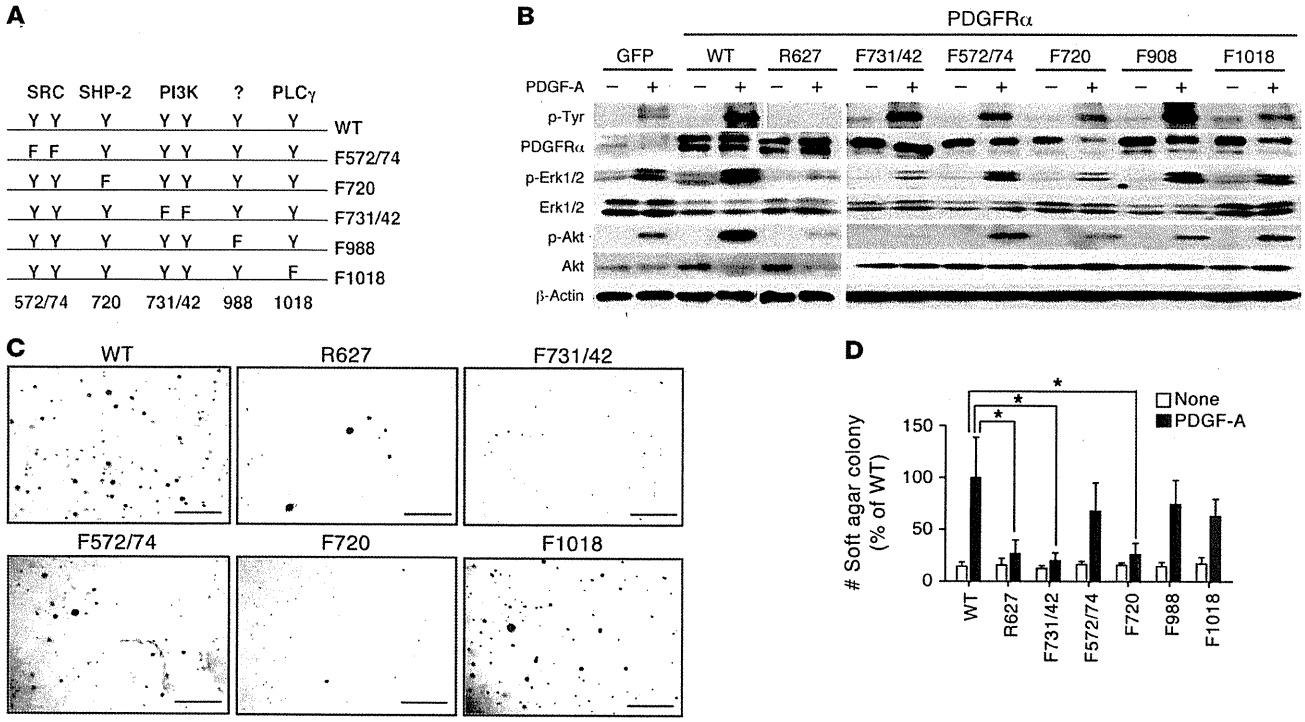

Figure 5

Impacts of PDGFRα mutations on downstream signaling of PDGFRα and anchorage-independent growth in soft agar of *Ink4a/Arf*$^{-/-}$ mAsts. (**A**) Schematics of various PDGFRα mutants. (**B**) IB analyses of PDGF-A–stimulated *Ink4a/Arf*$^{-/-}$ mAsts overexpressing individual PDGFRα mutants. Corresponding total proteins or β-actin were used as loading controls. Vertical lines in left panels of p-Tyr, PDGFRα, and β-actin indicate that these images were modified by removal of two lanes of samples between WT and R627. The longer white vertical line indicates that the samples were analyzed in separate SDS-PAGE gels due to the limit of sample loading per gel. (**C** and **D**) Soft agar assay. (**C**) Representative images of soft agar colonies. (**D**) Quantification of soft agar assays. Data are presented as mean ± SD and are representative of 2 independent experiments. Scale bars: 1 mm. *$P < 0.01$.

p-Erk1/2 in mAsts (Supplemental Figure 4C), also inhibited soft agar growth of these cells (Figure 5A), validating Erk1/2 as a mediator of PDGFRα–SHP-2 signaling. Taken together, these data demonstrate that the PDGFRα/PDGF-A–enhanced tumorigenicity of *Ink4a/Arf*-deficient mAsts and human glioma cells requires intact SHP-2 and PI3K enzymatic activities.

SHP-2 ablation disrupts PI3K/AKT/mTORC1/S6K activation and attenuates the enhanced tumorigenesis of PDGFRα-expressing mAsts. We then examined the impact of SHP-2 inhibitors (PHPS-1 and NSC87877) and PDGFRα-F720 on PI3K signaling. As shown in Figure 5B and Figure 8A, PDGFRα-F720 mutant and SHP-2 inhibitors significantly decreased PDGF-A–stimulated p-Akt in PDGFRα-expressing mAsts. A nearly complete knockdown of SHP-2 by siRNAs markedly reduced the stimulated p-Akt levels in these cells, possibly through interruption of the association between PI3K (p85 subunit) and PDGFRα (Figure 8B). However, a previous study showed that PDGFRα-F720 mutation did not result in a decrease in PI3K association with the RTK in mouse fibroblasts (10). Similarly, when SHP-2 was knocked down in NIH3T3 cells, a minimal impact of SHP-2 inhibition on PDGF-A–induced PI3K association and Akt phosphorylation was observed in these fibroblasts (Supplemental Figure 5A), suggesting that the impact of SHP-2 on PI3K association with the RTK and p-Akt in astrocytes and glioma cells was specific. To examine whether the effect of SHP-2 knockdown on p-Akt signaling was specific to PDGFRα signaling, we knocked down SHP-2 by siRNAs in EGFRvIII-expressing *Ink4a/Arf*$^{-/-}$ mAsts (WT PTEN) and LN444 and U87MG (both PTEN mutant) cells. We observed a reduction or a modest impact of p-AKT level in LN444/EGFRvIII and U87MG/EGFRvIII cells, respectively (Supplemental Figure 5B), suggesting that SHP-2 also regulates PI3K/AKT activation in other RTK signaling. However, Akt phosphorylation was absent in *Ink4a/Arf*$^{-/-}$ EGFRvIII mAsts, possibly due to the presence of WT Pten in these cells.

We next tested whether signaling downstream to Akt was affected by SHP-2 inhibition. We found that SHP-2 inhibitors (Figure 8A), SHP-2 siRNA knockdown (Figure 8B), or PDGFRα-F731/42 and PDGFRα-F720 mutations (Figure 8C) significantly impaired PDGF-A–stimulated phosphorylation of S6 kinase (p-S6K) downstream to the mammalian target of rapamycin (mTOR) pathway. Thus we further determined the impact of the ablation of SHP-2 and its downstream target the mTOR pathway on cell transformation. Strikingly, stable knockdown of SHP-2 by shRNAs markedly reduced PDGFRα-promoted soft agar growth of mAsts (Figure 8D). Additionally, treatment with mTOR complex 1 (mTORC1) inhibitor rapamycin led to a dose-dependent decrease in soft agar colonies formed by PDGF-A–stimulated *Ink4a/Arf*$^{-/-}$ mAsts expressing PDGFRα or LN444 cells (Supplemental Figure 6, A and B), compared with their respective DMSO-treated controls.

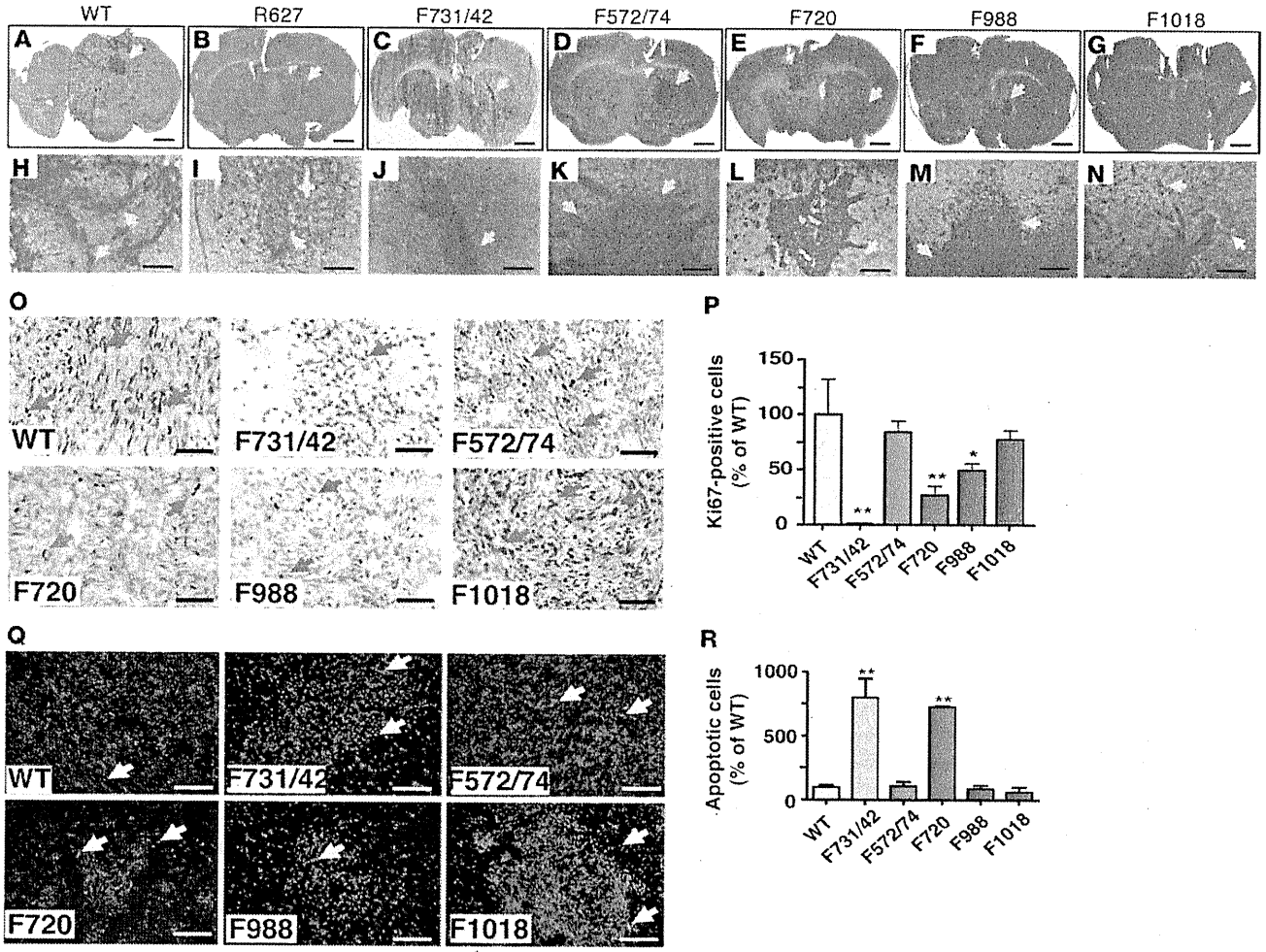

Figure 6

Impacts of individual mutations of PDGFRα in mAsts on brain tumorigenesis. (**A–N**) Representative H&E staining images of various brain sections from 2 independent experiments with at least 5 mice per group with similar results. Mice that received various types of cells displayed similar tumor onset and survival times as described in Figure 1. Brains were harvested 25–30 days (**A**), 30–35 days (**B**, **C**, **D**, and **G**), and 35–40 days (**E** and **F**) after transplantation. Scale bars: 1 mm (**A–G**), 200 μm (**H–N**). Arrows indicate tumors or invading cells. (**O**) Ki-67 staining of brain sections. Scale bars: 50 μm. Arrows indicate Ki-67–positive cells. (**P**) Quantification of Ki-67 staining. (**Q**) TUNEL staining images. Scale bars: 100 μm. (**R**) Quantification of TUNEL staining. Data in **P** and **R** are presented as mean ± SD. $^*P < 0.01$; $^{**}P < 0.001$.

Similarly, rapamycin was able to effectively suppress the cell transformation capacity conferred by EGFRvIII expression in these cells (Supplemental Figure 6C). Previous studies suggested that the limited efficacy of rapamycin in clinical use was due to the capacity of rapamycin to potentiate PI3K/Akt signaling (24). However, we did not observe an increase of p-Akt level in both *Ink4a/Arf*-deficient mAsts and LN444 cells treated with rapamycin up to 72 hours (Supplemental Figure 6D). These results suggest that PDGFRα-promoted tumorigenesis necessitates an intact SHP-2 activity that regulates the PI3K/AKT/mTOR pathway. Since, in clinical glioblastomas, constitutively active PI3K mutations are mostly observed in specimens with no *PDGFRA* aberrations (3, 4), we introduced a constitutively active PI3K p110 subunit (p110α-CAAX) into *Ink4a/Arf*$^{-/-}$ mAsts that either expressed PDGFRα-F720 or an SHP-2 shRNA. In both cell lines, we observed a rescue effect of p110α-CAAX in soft agar colony formation (Figure 8E), suggesting that PI3K/AKT/mTOR acts downstream of SHP-2 in PDGFRα-overexpressing gliomas, and that activating PI3K mutations in clinical gliomas might be able to bypass SHP-2 activation to promote tumorigenesis. Taken together, our results suggest that SHP-2 regulates the PI3K/AKT/mTOR signaling emanating from PDGFRα activation.

PDGFRα and PDGF-A are co-expressed, and their expression is linked with the activation of the SHP-2 and the PI3K/AKT/mTOR signaling in clinical glioblastomas. To determine whether PDGF-A and PDGFRα are co-expressed and whether there is a link of overexpression of PDGF-A and PDGFRα and activation of the SHP-2 and the PI3K/AKT/mTOR signaling in clinical glioma specimens, we performed IHC staining on a total of 158 paraffin-embedded primary human glioma specimens using anti-PDGFRα, anti-PDGF-A, anti-p-SHP-2 Tyr542, anti-p-AKT Ser473, and anti-p-S6 Ser235/236 antibodies. PDGFRα proteins were detected at medium to high levels in 17 of 87 GBMs (WHO grade IV tumors) and in 9 of 71 grade II and III tumors. Among these PDGFRα-positive gliomas,

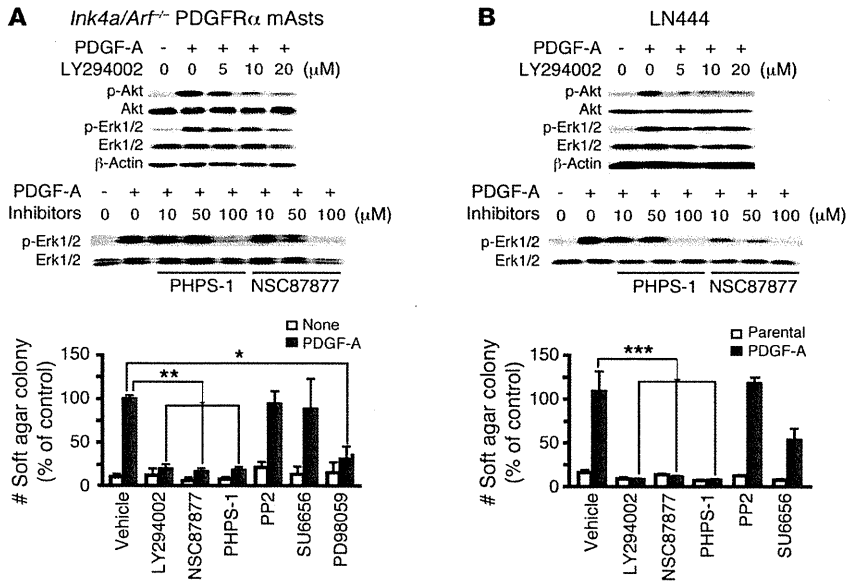

Figure 7
Inhibition of PI3K or SHP-2 activities suppresses PDGFRα-stimulated signaling and cell transformation. (**A**) Inhibitors of PI3K (LY294002), SHP-2 (PHPS-1 and NSC87877), and MEK (PD98059), but not SFK (SU6656 and PP2), abrogate cell transformation of PDGFRα-overexpressing *Ink4a/Arf*$^{-/-}$ mAsts. Top and middle: IB analyses. Bottom: Quantification of soft agar assays. Cells were grown in triplicate in soft agar with or without LY294002 (10 μM), PHPS-1 (100 μM), NSC87877 (100 μM), PP2 (5 μM), SU6656 (5 μM), or PD98059 (10 μM). (**B**) PI3K and SHP-2 inhibitors suppress PDGF-A–promoted soft agar growth of *INK4A/ARF*-deficient LN444 glioma cells. Top and middle: IB analysis. Bottom: Soft agar assays. Concentrations of the inhibitors and experimental conditions were identical to those in **A**. Data are presented as mean ± SD. For IB analyses, corresponding total proteins or β-actin were used as loading controls. All data are representative of 2 independent experiments. *$P < 0.001$; **$P < 0.0001$; ***$P < 0.01$.

PDGF-A was often co-expressed in the same population of tumor cells (Figure 9, B and C, and Supplemental Table 1). Significantly, phosphorylation of SHP-2 Y542 (p-SHP-2, required for activation of SHP-2) (25), AKT (p-AKT), and ribosomal S6 subunit (p-S6) was also often detected on sister sections of the same tumor in many of the PDGF-A/PDGFRα–positive glioma specimens (Figure 9, B–F, and Supplemental Table 1), suggesting a link between activation of PDGF-A/PDGFRα and stimulation of SHP-2, AKT, and mTOR in clinical glioblastoma specimens. To validate these data, we performed IB analyses on a separate cohort of a total of 20 snap-frozen clinical GBM specimens. As shown in Figure 9G, PDGFRα was expressed at high levels in 7 of 20 GBM samples, 5 of which expressed PDGF-A proteins, suggesting an autocrine PDGFRα signaling in these tumors. In 4 of these 5 PDGF-A/PDGFRα–positive tumors, p-AKT, p-SHP-2, and p-S6 were also detected. Of note, expression of PDGF-A, p-AKT, p-SHP-2, and p-S6 at various levels in other tumor samples likely reflects the impact of heterogeneous gene alterations such as mutations of PTEN, TP53, and overexpression of EGFR/EGFRvIII and c-MET that affect the expression or activation (phosphorylation) of these proteins in clinical glioblastomas. Taken together, these results establish a link of PDGF-A/PDGFRα expression with activation of SHP-2 and PI3K/AKT/mTOR signaling in clinical glioblastoma samples.

Discussion

In this study, we report that PDGFRα and/or PDGF-A overexpression is able to drive gliomagenesis of *Ink4a/Arf*-deficient mAsts and human glioma LN444 and LN443 cells. Re-introduction of p16INK4a but not p19ARF into *Ink4a/Arf*-null mAsts suppresses PDGFRα-promoted tumor growth. In the absence of PI3K or SHP-2 signaling, PDGFRα fails to enhance tumorigenesis in the brain of mice. Additionally, we establish a link between activation of SHP-2 and the PI3K/AKT/mTOR signaling in PDGFRα-stimulated tumorigenesis in vitro, in mice, and in clinical glioblastoma specimens. Therefore, our data demonstrate that co-alteration of the RTK PDGFRα and tumor suppressor p16INK4a is required for gliomagenesis and that SHP-2 is a critical linker between the PI3K/AKT/mTOR pathway and PDGFRα in the formation of gliomas.

A unique feature of this study is that specific activation of PDGFRα signaling in vivo by PDGF-A, a ligand that binds to PDGFRα but not PDGFRβ (14) as an autocrine loop significantly enhanced the tumorigenesis of *Ink4a/Arf*-deficient mAsts and human glioma cells in the brain. Early studies of clinical glioma specimens showed that PDGF-A and PDGFRα are overexpressed in tumor cells, while PDGF-B and PDGFRβ are expressed in hyperplastic capillaries, suggesting both autocrine and paracrine loops for PDGF/PDGFR activation in gliomas (15). In neonate and adult mice, expression of PDGF-B induces de novo gliomas from GFAP-positive astrocytes and nestin-expressing glial progenitor cells through activation of PDGFRα and PDGFRβ in the brain of both WT and *Ink4a/Arf*-deficient animals (26, 27). Moreover, in WT *Ink4a/Arf* mice, infusion of PDGF-A proteins into the lateral ventricle stimulated tumor-like growth of PDGFRα-positive NSCs in the SVZ in the brain (17). Importantly, data from The Cancer Genome Atlas (TCGA) and other studies revealed that PDGFRα is overexpressed and amplified and often co-expressed with PDGF-A in clinical glioblastoma samples (3, 28, 29). Our results not only functionally validated these studies but also further demonstrated the significance of specific activation of PDGFRα signaling by PDGF-A in cooperation with loss of p16INK4a but not p19ARF in promoting gliomagenesis. We found that when PDGFRα signaling is activated in *Ink4a/Arf*$^{-/-}$ mAsts or human glioma cells, mice that received these cells developed significantly larger and highly invasive tumors in the brain. In contrast, no enhancement of tumorigenesis was found in mice that received glioma cells with PDGFRα and an intact *CDKN2A* locus (19). Together, our studies indicate that PDGFRα activation together with *Ink4a/Arf* loss results in enhanced tumor growth of both mAsts and human glioma cells in the brain.

Tumor suppressor P16INK4A is frequently mutated in clinical glioblastomas (3, 4, 29). In mice, loss of p16INK4a and p19ARF was shown to be indispensable in facilitating tumorigenesis (6). *Ink4a/Arf*-deficient mice were viable and developed spontaneous

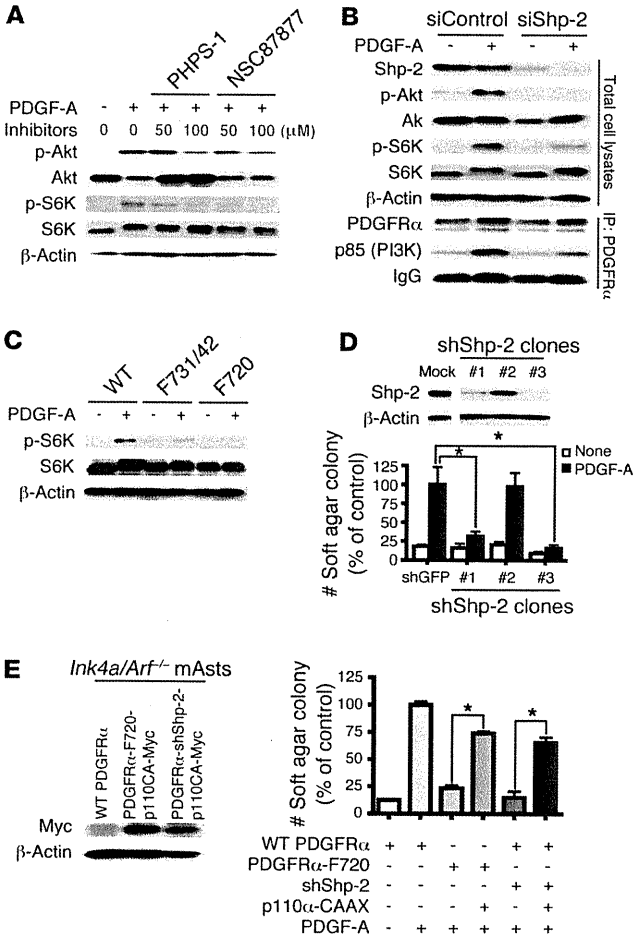

Figure 8

SHP-2 recruits PI3K to activate AKT/mTOR/S6K pathway in PDGFRα/PDGF-A–mediated tumorigenesis. (**A**) IB analyses of serum-starved *Ink4a/Arf*$^{-/-}$ PDGFRα-expressing mAsts treated with SHP-2 inhibitors PHPS-1 or NSC87877 for 24 hours followed by 50 ng/ml PDGF-A for 5 minutes. (**B**) IP/IB analysis of PDGFRα-overexpressing mAsts that were transfected with SHP-2 siRNA for 48 hours and serum starved for an additional 24 hours, followed by PDGF-A stimulation. (**C**) IB analysis of phospho-S6 kinase levels of various mAsts stimulated by PDGF-A. (**D**) SHP-2 shRNAs suppressed soft agar growth of mAsts. Top: IB analysis. Bottom: Clones that had a significant decrease in SHP-2 expression (#1 and #3 in top panel) showed reduced tumor cell growth in soft agar. Data are presented as mean ± SD. $^*P < 0.01$, Student's *t* test. (**E**) Constitutively activated PI3K rescued the inhibitory effect of SHP-2 inhibition on blocking PDGFRα-mediated cell transformation. Left: IB analysis of expression of p110α-CAAX. Right: Soft agar assays. Data are presented as mean ± SEM. $^*P < 0.0001$. For all IB analyses, corresponding total proteins, β-actin, or total pulled-down IgG were used as loading controls. All data are representative of 2 to 3 independent experiments.

tumors at early ages, but without detectable tumors in the brain (6, 7). Further studies showed that *Ink4a/Arf* loss cooperates with oncogenic K-Ras, EGFRvIII, or PDGF-B expression in promoting gliomagenesis in the brain (7, 8, 16, 26, 27). However, compared with p16INK4a loss, which contributes to tumor initiation from mAsts, p19ARF deficiency was shown to display a more pronounced impact on cell transformation and gliomagenesis (30, 31). Our data corroborate and also differ from these studies. We showed that re-expression of p16INK4a but not p19ARF in PDGFRα-expressing *Ink4a/Arf*$^{-/-}$ mAsts inhibited tumorigenesis. Inhibition of CDK4/6, the direct target of p16INKa by a specific inhibitor (20), in *Ink4a/Arf*$^{-/-}$ mAsts and glioma cells attenuated PDGF-A stimulation of soft agar growth, suggesting that CDK4/6/p-RB signaling is required for PDGFRα-induced tumorigenesis. On the contrary, although p53 was functional in *Ink4a/Arf*$^{-/-}$ PDGFRα-expressing mAsts, p19ARF was unable to suppress soft agar growth of these cells. Since p19ARF derepresses p53 signaling while PI3K/Akt activates p53 E3 ubiquitin ligase Mdm2 (32), it is plausible that the robust PI3K/Akt activation in PDGFRα-overexpressing cells triggers Mdm2-mediated p53 degradation and thereby renders tumorigenic mAsts resistant to p19ARF inhibition (21). It is also likely that loss of p19ARF is required for survival of glioma cells under certain situations, such as treatment of DNA damage–inducing agent CDDP (Supplemental Figure 3). At least during the initiation or maintenance of cell transformation, p19ARF loss appears to be dispensable (30, 31), since knockdown of *INK4A* alone in WT *INK4A/ARF* LN319 glioma cells restored PDGFRα stimulation of anchorage-independent growth in soft agar. Taken together, these data suggest that loss of p16INK4a plays a predominant role in PDGFRα-promoted gliomagenesis.

The third important aspect in this study is that we functionally assigned signal modules of PDGFRα in promoting gliomagenesis and tumor invasion in the brain of mice. Previous studies by uncoupling individual signaling pathways from PDGFRα using a series of F-to-Y mutants revealed unequal contributions of each signaling pathway emanating from PDGFRα activation (11, 12, 14). Our in vivo and biochemical data corroborate these reports. When compared with WT PDGFRα overexpression, loss of intrinsic tyrosine kinase activity (R627) of the RTK or binding capacity to PI3K (F731/42) or SHP-2 (F720) abrogated PDGFRα-promoted gliomagenesis, thus signifying the central roles of PI3K and SHP-2 signaling in PDGFRα function. However, while disruption of PDGFRα association with SFKs (F572/74) or PLCγ (F1018) only had a moderate impact on tumor formation in the brain, significant inhibition of tumor cell infiltration in the brain was seen in these tumors, as compared with the WT PDGFRα tumors, thus validating the role of SFKs and PLCγ in mediating PDGFRα-stimulated cell invasion (10). Moreover, a separate set of experiments with individual "add-back panel" mutants in

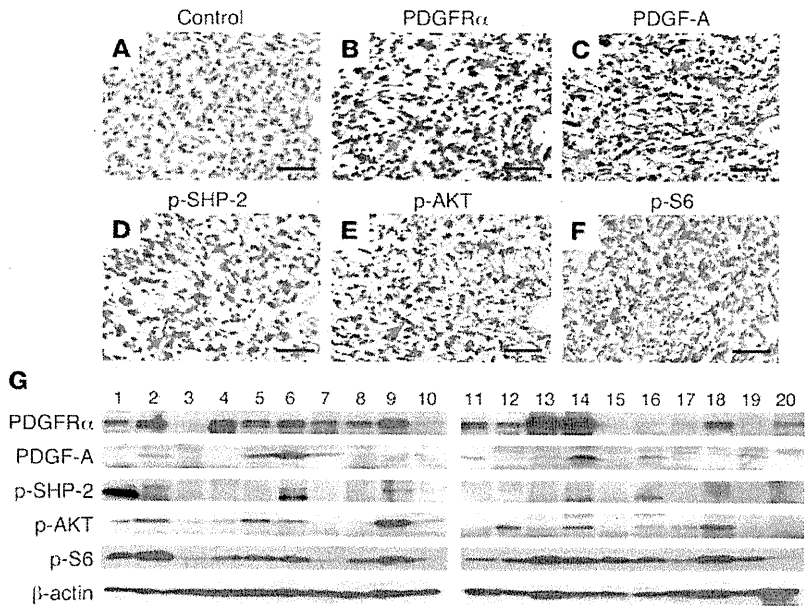

Figure 9
PDGFRα and PDGF-A are co-expressed in clinical glioma specimens with activated SHP-2 and PI3K/AKT/mTOR pathways. (**A–F**) Images of IHC staining on sister sections of a representative human J212 GBM specimen, using anti-PDGFRα (**B**), anti–PDGF-A (**C**), anti–p–SHP-2 (Y542) (**D**), anti–p-AKT (**E**), and anti–p-S6 (**F**) antibodies. (**A**) No primary antibody. Arrows indicate positive staining for the indicated proteins. Scale bars: 50 μm. (**G**) IB analysis of tissue lysates of a separate cohort of 20 human GBM snap-frozen specimens using indicated antibodies. β-Actin was used as a loading control. Data are representative of 2 independent experiments with similar results.

which 1 of 5 signal modules was individually retained as single or double Y residues (Y731/42, Y572/74, Y720, Y988, and Y1018) could not fully restore PDGFRα-promoted tumorigenesis in the brain (data not shown), consistent with the previous findings using an identical set of PDGFRα add-back panel mutants (10). It is plausible that, similar to this previous in vitro study (10), in which retention of a combination of 2 or 3 add-back signaling modules with comparable levels of total RTK protein in WT PDGFRα–expressing cells was able to restore PDGFRα-mediated biological responses, co-activation of PI3K (Y731/42)– and SHP-2 (Y720)–mediated signaling may be required for the full spectrum of WT PDGFRα–promoted gliomagenesis in the brain.

The last (and what we believe is also the most novel) finding in this study is the emergence of SHP-2 as an essential mediator in PDGFRα-promoted gliomagenesis. SHP-2 (encoded by *PTPN11* gene) is a protein tyrosine phosphatase (PTP) identified as a bona fide proto-oncogene that activates Ras/MAPK signaling through a yet-to-be-defined mechanism (33). Additionally, the role of SHP-2 in mediating PDGFRα signaling has not been clear (9, 11, 14). In human cancers including GBMs, mutations of SHP-2 or its binding partners have been reported, leading to sustained Ras/MAPK signaling (34, 35). Recent genomic analysis of TCGA data has designated *PTPN11* as one of the 6 "linker" genes, which are statistically enriched for connections to various GBM altered genes, thus suggesting a critical role for SHP-2/*PTPN11* in modulation of downstream biological signaling in gliomagenesis (36). Our data not only establish the critical role of SHP-2 in mediating PDGFRα activation for glioma formation but also functionally validate this hypothesis. We showed that inhibition of SHP-2 function by removal of its binding module in PDGFRα (F720 mutant), gene knockdown or pharmacological inhibitors significantly impaired PDGFRα stimulation of tumorigenesis in vivo and in vitro and its downstream signaling effectors, Erk1/2 and PI3K/Akt/mTOR in *Ink4a/Arf*-deficient mAsts and glioma cells. Significantly, re-expression of a constitutively active p110, the catalytic subunit of PI3K, rescued the inhibition of SHP-2 in *Ink4a/Arf*-deficient mAsts. In EGFRvIII-expressing U87MG glioma cells, SHP-2 regulates activities of ERK/2 and CDC2 that modulate cell cycle progression but has a minimal effect on AKT activation (23). On the contrary, we found that knockdown of SHP-2 not only attenuated PDGFRα stimulation of Erk1/2 activity but also impaired PI3K/Akt/mTOR activity in *Ink4a/Arf*-deficient mAsts and human glioma cells. The impact of inhibition of SHP-2 on PI3K/Akt signaling appears to be specific in astrocytic tumors, since we did not observe inhibited PDGF-A stimulation of p-Akt or association of PI3K with PDGFRα in SHP-2–knockdown NIH3T3 fibroblasts. On the other hand, the MEK inhibitor PD98059 also reduced the tumorigenicity of *Ink4a/Arf*-deficient mAsts, indicating that SHP-2–mediated PDGFRα signaling requires not only PI3K/Akt but also Erk1/2 activation in gliomagenesis. Additionally, SHP-2 was found to either positively or negatively regulate PI3K/AKT activity (34). However, in our model systems, SHP-2 is required for full activation of PI3K/Akt/mTOR, and inhibition of mTOR by rapamycin markedly suppressed PDGFRα-promoted tumorigenesis. These data are significant since a recent proteomic study revealed that mTOR signaling is predominantly activated in "*PDGFRA* co-cluster" glioblastomas (37), thus corroborating our observations. However, since phosphorylation of Akt Ser473 occurs both upstream and downstream of mTORC2 signaling, our data do not rule out the role of mTORC2 in PDGFRα-activated signaling. Lastly, our data also demonstrated the importance of activation of PI3K/mTOR signaling by SHP-2 in PDGFRα- or EGFRvIII-promoted tumorigenesis. Taken together, our findings suggest SHP-2 as a critical modulator that regulates PDGFRα-mediated PI3K/AKT/mTOR activities in the development of malignant glioblastomas.

In summary, this study provides molecular insights into the mechanisms by which *PDGFRA* amplification together with loss of *INK4A/ARF* promotes gliomagenesis in the brain. Our data identified SHP-2, as well as PI3K, as a pivotal mediator of PDGFRα signaling in glioma formation. These results have direct clinical relevance, since we not only establish a model system to demonstrate the co-operative role of *PDGFRA* overexpression and *INK4A/ARF* loss in clinical glioblastomas, but also provide functional evidence to validate genomic analyses demonstrating that SHP-2/*PTPN11* is an essential "linker" among glioma altered genes (36). Secondly, activated mTOR